Spatio-temporal characteristics of heavy precipitation events observed over the last decade on the eastern French Mediterranean coastal area

Sarah Vigoureux, Pierre Brigode, Maria-Helena Ramos, Julie Poggio, Raphaëlle Dreyfus, Emmanuel Moreau, Christophe Laroche, Emmanuel Tric

Journal of Hydrology: Regional Studies 56 (2024) 101988

Contents lists available at ScienceDirect

Journal of Hydrology: Regional Studies

journal homepage: www.elsevier.com/locate/ejrh

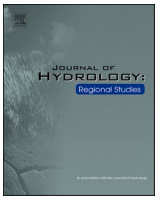

Spatio-temporal characteristics of heavy precipitation events observed over the last decade on the eastern French Mediterranean coastal area

Sarah Vigoureux [a,b,e,*], Pierre Brigode [a,c,d,e], Maria-Helena Ramos [c,e], Julie Poggio [b,e], Raphaëlle Dreyfus [b,e], Emmanuel Moreau [e,f], Christophe Laroche [e,g], Emmanuel Tric [a,e]

[a] Université Côte d'Azur, CNRS, OCA, IRD, Géoazur, France
[b] SMIAGE Maralpin, Nice, France
[c] Université Paris-Saclay, INRAE, HYCAR, Antony, France
[d] Univ Rennes, CNRS, Géosciences Rennes - UMR 6118, Rennes F-35000, France
[e] Université Côte d'Azur, CNRS, LJAD, France
[f] BOWEN, NOVIMET, France
[g] Météo-France, Direction Interrégionale Sud-Est, Aix-en-Provence, France

ARTICLE INFO

Key words:
Heavy precipitation
radar rainfall
river discharges
mediterranean events

ABSTRACT

Study region: eastern part of the French Mediterranean coastal area.
Study focus: This work focuses on the heavy precipitation events that have affected the eastern part of the French Mediterranean coastal area over the last decade and the river discharges associated with these events. The aim is to make a throughout analysis of the spatio-temporal characteristics of heavy precipitation events, and to evaluate whether a high flow event is associated with them when looking at river discharges on affected catchments.
New hydrological insights for the region: Based on radar-based precipitation grids, 158 heavy precipitation events (HPEs) affected the study area over the period 2007–2020. In addition, 65 % of HPEs were associated with a high flow event (HFE) on one or more gauged catchments. Results show that HPEs were more frequent during the beginning of summer and autumn. A large portion of autumn and winter HPEs were associated with a HFE. Looking at the spatio-temporal characteristics of the HPEs, their mean duration was 20 hours, with 42 % of the events lasting less than 6 hours. Some common characteristics among the HPEs that caused HFEs were identified: all HPEs lasting more than 30 hours and all HPEs with catchment precipitation accumulation above 150 mm were associated with a HFE.

Abbreviations: HPEs, Heavy Precipitation Events; HFEs, High Flow Events.

* Corresponding author at: Université Côte d'Azur, CNRS, OCA, IRD, Géoazur, France.
E-mail address: sarahvigoureux@gmail.com (S. Vigoureux).

https://doi.org/10.1016/j.ejrh.2024.101988
Received 16 April 2024; Received in revised form 20 September 2024; Accepted 22 September 2024
Available online 3 October 2024

1. Introduction

1.1. Heavy rainfall and flooding in the Mediterranean region

Despite its generally sunny and nice climate on the Mediterranean coast, the municipalities in this region are particularly exposed to heavy rains and frequently affected by floods (Gaume et al., 2016), resulting in significant human and material losses. Notable recent examples include the Daniel storm in September 2023, which led to catastrophic flooding in Greece and two dam breaks in Lybia, causing 11,000 casualties and extensive damages (Qiu et al., 2023). Heavy precipitation events on the Mediterranean coastal area can be explained by its proximity to the Mediterranean Sea. The Mediterranean Sea is an important water reservoir from which wet air masses rise by meeting the hot air above the coastal cities, which favors intense convection phenomena, leading to short but heavy and localized rainfall. Wet air masses coming from the sea can also be driven upwards confronted with the local relief, leading to stationary and sometimes heavy orographic rainfall (Boudevillain et al., 2009; Drobinski et al., 2013; Ducrocq et al., 2014).

In France, the Cévennes mountain range has been particularly studied over the past decades due to the remarkable intensity of the rainfall events affecting this region (Berne et al., 2009; Ceresetti, 2011; Ceresetti et al., 2012; Emmanuel et al., 2015), known as “Cévenol episodes”. This term is used instead to designate orographic precipitation in shallow convection meteorological situations and is a special case of the "Mediterranean episodes", which also include deeper convection events affecting the entire French Mediterranean coast and the Alps (Molinié et al., 2012; Rysman et al., 2016; Mélèse et al., 2018).

1.2. Impacts on eastern part of the French Mediterranean coastal area

In recent years, the Southeast of France has been affected by several catastrophic floods, often caused by rapid river responses to heavy rainfall. While the 2015 and 2019 floods mainly impacted the coastal area of the Var and Alpes-Maritimes French departments (Brigode et al., 2021), the Alex and Aline storms, in 2020 and 2023, affected inland areas above Nice (Payrastre et al., 2022), showing the important spatial variability of rainfall in this region.

During the October 2015 flood, stationary and highly intense rainfall affected the coastal part of southeastern France, with 160 mm recorded in less than 2 hours in Cannes, causing flooding of several rivers and resulting in catastrophic human and material losses (20 victims and €600 million of damage insured). The Alex storm in October 2020 brought 80–100 mm of rain in 1 hour, with total rainfall exceeding 600 mm in 24 hours in the Vésubie and Roya valleys, causing. flooding as well as mudslides and landslides (Chmiel et al., 2022), 18 deaths and around one billion euros in material damage (IGEDD, 2023). Floods were also observed in November 2019 while the hourly rainfall accumulation was not exceptionally intense, but the daily rainfall accumulation was high, with, for example, nearly 400 mm between 22 and 24 November above Mandelieu, causing again heavy human and material losses (9 fatalities and €390 M in insured losses).

Thus, the Southeast of France faces significant heavy precipitation hazards, with complex and varied consequences. Recent events have highlighted substantial differences in rainfall intensity, duration, and the regions impacted. These variations emphasize the need for detailed analysis to effectively manage and mitigate the risks associated with heavy precipitation in this region. Furthermore, recent studies of daily and sub-daily changes in heavy precipitation over the Mediterranean area have shown that heavy precipitation events will potentially become more frequent, with an expected increase of the mean and the maximum precipitation intensities (Tramblay and Somot, 2018; Ribes et al., 2019), as well as an increase of the surface of the impacted area, especially in the Southeast of France (Caillaud et al., 2023).

1.3. On the need of dedicated high-resolution hydrometeorological analysis

As mentioned by Breugem et al. (2020), hydrometeorological analyses give keys to better understand the causes and the development of a flood event, as well as the hydrological response of catchments to precipitation events, which may help in the anticipation of floods and the associated losses. In this context, some studies have analyzed trends on heavy precipitation intensity over the south of France using rain gauges observations over a long period of time (Blanchet et al., 2016; Ribes et al., 2019), but without looking at the duration and spatial characteristics of the heavy precipitation events. Heavy precipitation spatial and temporal characteristics have been mostly studied over shorter periods of time, focusing on single precipitation events that lead to catastrophic flood events (Delrieu et al., 2005; Drobinski et al., 2013; Garambois et al., 2014; Boudou et al., 2016; Gilabert and Llasat, 2018; Brigode et al., 2021; Chochon et al., 2021). Another approach consists in studying all the observed heavy precipitation events that affected an area, no matter if it has caused floods or not. For instance, Ricard et al. (2012) collected 305 precipitating systems with daily precipitation totals above 150 mm that occurred on southern France over the 1967–2006 period using the rain gauges observations. They looked at the yearly and seasonal distribution of the number of HPEs as well as daily maximum precipitation values and the main characteristics of the atmospheric conditions just before the precipitating system. Lengfeld et al. (2021), studied more than 20,000 heavy precipitation events that affected Germany over a 20–year period (2001–2020) using radar-based rainfall data. They made a catalog (called CatRaRE for Catalog of Radar-based heavy Rainfall Events) of heavy precipitation events and their characteristics describing the meteorological conditions and including a geographical and demographic description of the area impacted by the heavy precipitation. This catalog is designed to be useful for hydrologists, climatologists, and professionals involved in risk management. In their study, they did not look at the reactions of the rivers to these heavy precipitation events. Inspired by their work, we present a method to collect and study the spatial and temporal characteristics of all the heavy precipitation events that affected Southeast France during the last decade. In

addition, we use the river discharges associated with these heavy rainfall events in order to identify which heavy precipitation events can be associated with high flow events. By doing so, we can compare the characteristics of heavy precipitation events that caused high flow events with those that did not.

1.4. Objectives of this study

The objectives of this study are to take advantage of the hourly radar-based precipitation database COMEPHORE (Tabary et al., 2012) in France (i) to apply an automatic selection method inspired by Lengfeld et al. (2021) to collect all the heavy precipitation events that affected the eastern part of the French Mediterranean coastal area during the last decade; (ii) to compute and summarize spatial and temporal heavy precipitation characteristics variability at the hourly scale; and (iii) to identify what are the common characteristics of heavy precipitation events leading to high flow events on gauged catchments in the study region. Short-duration precipitation events are studied as well as longer ones (from 1 h to a few days). Heavy precipitation intensities and spatial characteristics are studied at the COMEPHORE grid cell scale ($1 \times 1\ km^2$) as well as at the catchment scale (catchment sizes range from $18\ km^2$ to $2800\ km^2$). Finally, the subset of heavy precipitation events that caused high flow events over 36 gauged catchments are identified using the available discharge observations. The questions that will be discussed in this paper are:

- When (which season) do heavy precipitation events more often occur in the eastern part of the French Mediterranean coastal area?
- Where do heavy precipitation events more often occur?
- How long do the heavy precipitation events last?
- At the catchment scale, are there some common characteristics to the heavy precipitations with high flow events?

This paper is organized as follows: first, the study area as well as the precipitation and the discharge data used are described in Section 2; then the method used in order to select and characterize heavy precipitation events is presented in Section 3; in Section 4, the results are presented; finally, Section 5 presents the discussion, and Section 6 summarizes the conclusions.

2. Studied area and data

2.1. Studied area

The study area is the eastern part of the French Mediterranean coastal area (noted MedEst area hereafter) shown on Fig. 1a. It is extending from l'étang de Berre to the Italian border. Elevations are higher in the eastern part, with the Southern Alps reaching a maximum of 3000 m a.s.l. (Fig. 1b). The MedEst area covers a total area of $10{,}600\ km^2$. This area can be divided into 37 downstream coastal catchments with areas larger than $10\ km^2$. On these coastal catchments, meteorological stations and radars have been installed to measure and estimate precipitation over the area (meteorological radars are illustrated by red stars in Fig. 1b). In addition, water level gauging stations have been installed (illustrated by the black dots on Fig. 1b). The distribution of the surface areas of the 36 gauged catchments studied in this paper is given in Fig. 1c (the method used for the catchment delineation is described in Section 2.4). Places that are the most vulnerable to the risk of floods within the region are the urbanized and industrial areas. On the eastern half of the study area, the urbanized areas are located mainly on the coastal area, with an important industrial area on the downstream banks of the Var River (catchment id n°28), near the city of Nice. The remaining part of the study area is urbanized over its entire surface, with large coastal cities (Marseille, Toulon, Hyères, Saint-Raphaël). The names and outlet coordinates of the gauged catchments are given in Appendix 1.

In addition, the studied area is characterized by karstic sub-regions illustrated by the pink hatched areas in Fig. 1d. These karstic areas cover all or part of some of the gauged catchments studied. These karsts can have a significant hydrological impact on the infiltration, storage and sharing of water between catchments. Thus, it may influence the reactions of rivers when precipitation falls over the karstic area. The surface area of the catchment covered by karsts is shown in Fig. 1e. Some catchments (particularly those located to the west of the study area) are almost completely covered by karstic areas (more than 90 % of the surface of catchments n°1, 2, 3, 4, 5, 6, 7, 8, 9, 16, 22, 29, 32 is covered by karstic areas). On the contrary, some basins are almost not covered by karstic areas (less than 10 % of the surface of catchments n°19, 21, 25, 28, 31, 35 is covered by karstic areas), others are partially covered.

2.2. Precipitation data

The precipitation data used for this study come from the COMEPHORE (COmbinaison en vue de la Meilleure Estimation de la Précipitation HOraiRE, Tabary et al. 2012) database, computed and distributed by Météo-France. It is available at an hourly time step and 1 km x 1 km spatial resolution over France, from 1997 to 2020 without any missing value. This database is produced afterwards (not in real time) from radar-based precipitation estimates merged with previously validated rain gauges observations by kriging with external drift. There are no missing values in the COMEPHORE precipitation estimates because, as it is produced afterwards, any radar data that may be missing due to the unavailability of radar data (shutdowns for maintenance or breakdowns) or to masks (altitudes, obstructions to radar beams) are filled in the radar mosaic using precipitation estimates from neighboring radars as well as observations from ground-based rain gauges. Some radar estimates of the precipitation rates are also given above the sea and beyond the Italian border over a stretch of around 15–20 km.

The production method for this database has evolved over time, so in order to work with a homogeneous database regarding the

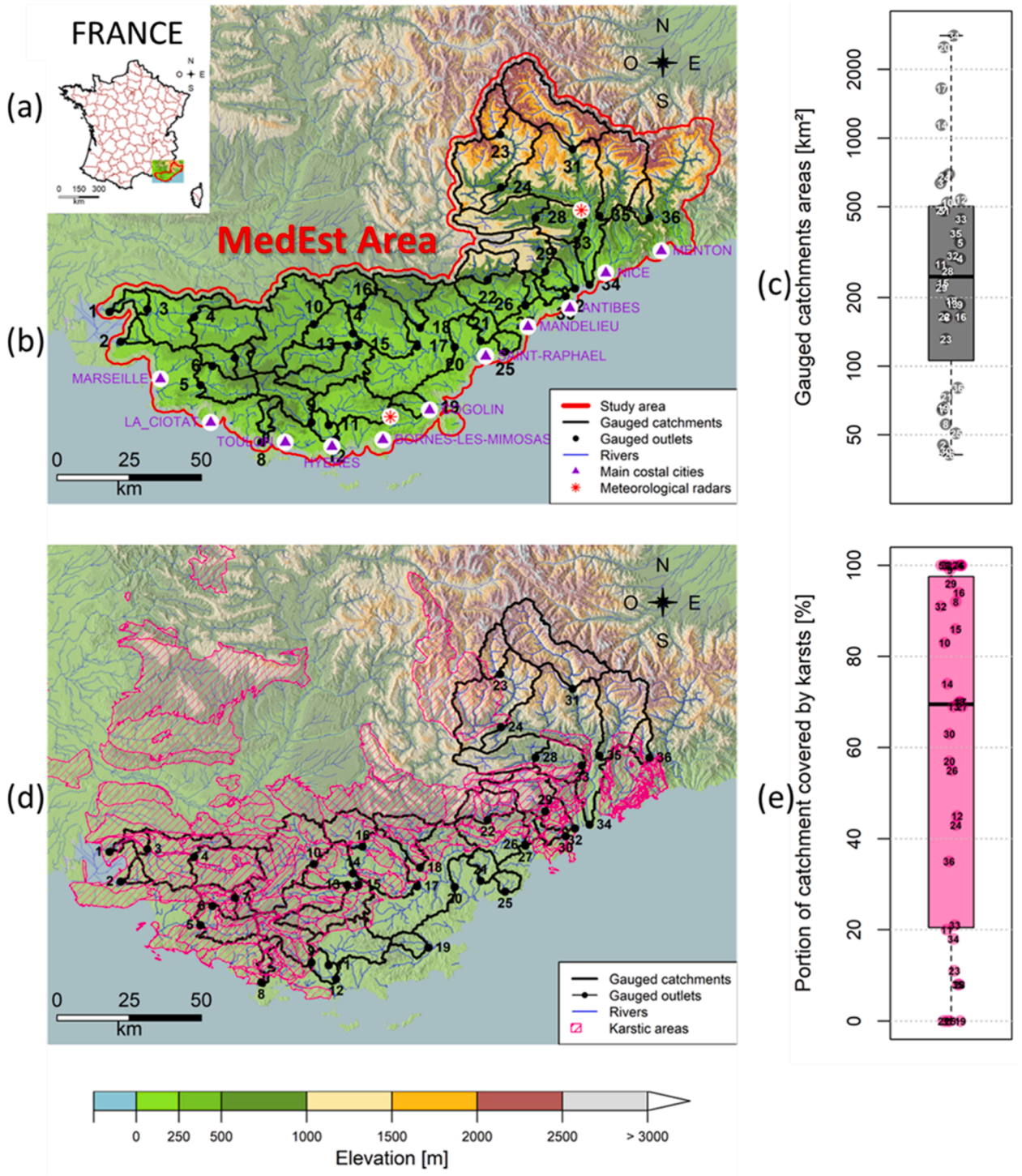

Fig. 1. (a) location of the study area in France; (b) location of the gauged outlets (black dots) and delineation of the gauged catchment areas (in black). The red outline illustrates the area defining the overall study area (MedEst area). The elevation shown in the background comes from the EU-DEM (EEA, 2016). Boxplot (c) illustrates the area distributions of the 36 gauged catchment surface areas. Map (d) illustrates the gauged catchments (in black) and karstic areas (in pink, from BD LISA). Boxplot (e) shows the portion of gauged catchments covered by karsts. The boxplots are built from the minimum, 25 %, 50 %, 75 % quantiles and the maximum.

precipitation rate computation, only data from the period 2007–2020 are used in this study. Two radars are installed over the eastern part of the Mediterranean coast, shown in red Fig. 1b. The first one, at Collobrières (S-band), has been operational since 2007, and the second one, an X-band radar, was installed on the Mont-Vial (above Nice) by NOVIMET (now BOWEN) in 2007 but data collected by this radar have only been used by Météo-France to compute radar precipitation estimates since 2017. Before 2017, precipitation estimates over the studied area are produced using the Collobrières radar estimates and kriging of rain gauges observations. The quality of the COMEPHORE database has improved over time with the incorporation of new radars and rain gauges data, but it still does not take into account altitudes to correct the orographic precipitation estimates (Caillaud et al., 2021). As these precipitation estimates are used to define the heavy precipitation events' dates, some heavy precipitation events may be missed in the analysis because of wrong precipitation estimates in the COMEPHORE data.

2.3. River discharges and catchment area delineation

Over the study area, most of the small coastal catchments (< 30 km^2) are ungauged. However, several water level gauging stations exist and enable real-time monitoring of instantaneous water levels. If a rating curve is also available, the calculation of river discharges is also possible for these stations. In this study, gauging stations locations and hourly river discharge data were directly obtained from the French platform HydroPortail (Dufeu et al., 2022). Fig. 1b shows the position of the 36 gauging stations used in this study. The criteria adopted was that all stations should have discharge data over the study period (2007–2020). Some missing discharge data can also lead to an underestimation of the number of HPEs with HFEs.

2.4. Catchment delineation

The upstream areas of the gauged catchments are shown with black lines in Fig. 1. The delineation of the catchments was computed from the EU-DEM (EEA, 2016), available at the 25 m resolution, and using the TauDEM tools (Tarboton, 1989). First, the flow directions and the areas drained by each DEM cell were defined. Then, a theoretical river network was defined using a threshold of a minimum drained area at 1000 cells of 25 m x 25 m (which represents an area of 0.625 km^2). Finally, each station was manually relocated on this theoretical river network in order to estimate the delineation of the associated topographic catchment.

It is important to note that this method is highly dependent on the quality of the DEM and the grid cell on which the station defining the outlet is positioned. By positioning the outlet a few cells downstream or upstream, one can add or remove a tributary from the catchment area and, therefore, significantly change the surface area of the catchment. In this study, each catchment delineated was quality-checked before their use in the analysis. Fig. 1c shows the distribution of the areas of the 36 gauged catchments selected.

3. Methodology

The general methodology adopted in this work can be summarized in three steps, which are detailed in the following subsections:

1. Selection of heavy precipitation events (Section 3.1);
2. Calculation of spatial and temporal characteristics of the heavy precipitation events (Sections 3.2 and 4.1, characteristics are summarized on Fig. 2);
3. Comparison of the characteristics of the heavy precipitation events that generated or did not generate high flow event (Section 4.3).

Fig. 2 (graphical abstract) summarizes this work. On the left part, the selection of heavy precipitation events is illustrated as well as the precipitation and the river discharges for one particular catchment (here the Loup at Villeneuve-Loubet Catchment n°29), because precipitation is studied on the whole study area as well as the catchment scale. On the right part, the objectives and the characteristics of the heavy precipitation events are summarized. The bottom part highlights the main conclusions.

3.1. Definition of a heavy precipitation event (HPE)

Although there does not appear to be a single widely used methodology for classifying precipitation events, most methods for selecting and studying heavy precipitation events are based on precipitation thresholds and a minimum duration between events. For example, Armon et al. (2020) defined a heavy precipitation event over the eastern Mediterranean area by considering precipitation exceeding a quantile-based threshold for each radar pixel, and precipitation accumulations over durations ranging between 1 and 72 h. They defined the precipitation threshold as the 99.5th quantile of the hourly precipitation observed in each radar pixel that was greater than 0.1 mm and storms are at least separated by 24 hours. Lengfeld et al. (2021) defined heavy precipitation over Germany in two ways: (i) based on the exceedance of one of 11 precipitation intensity thresholds (based on the precipitation thresholds defined by the German Meteorological Service's Severe Weather Alert Level 3) and (ii) based on the 5-year return period precipitation threshold over a sufficiently large area depending on the HPE duration D (9 km^2 for HPE lasting less than 3 hours and D*3 km^2 for longer HPE). They also defined a minimum period without precipitation between events also depending on the HPE duration: the temporal gap between two events is set as the minimum of the HPE durations and at least 4 hours. For instance, for two events with D1 = 12 h and D2 = 24 h durations, the minimal gap between the two events must be max(min (D1,D2), 4) hours, so 12 hours. To study heavy precipitation events projected by climate models over the eastern part of the French Mediterranean coast, Caillaud et al. (2021) considered precipitation events with at least one 3-km grid cell of a studied precipitation product (reanalysis or model output) above different

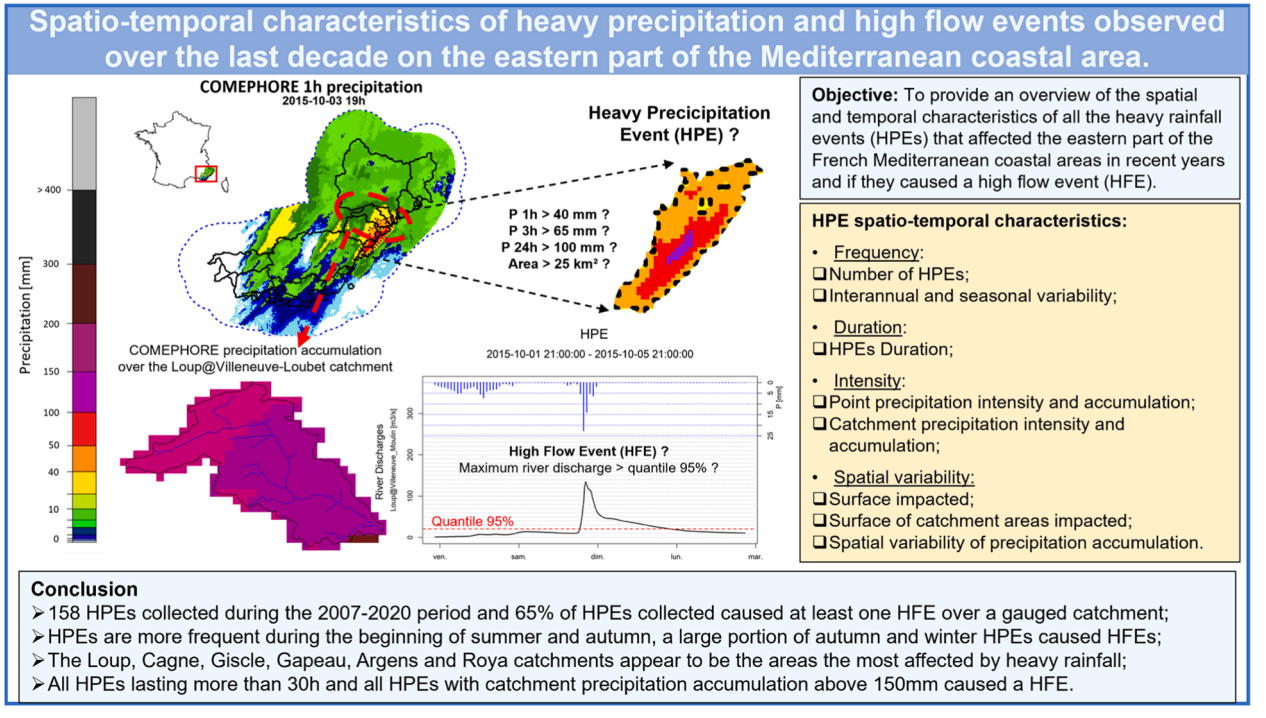

Fig. 2. the graphical abstract illustrates the objectives, the methodology and the main conclusions.

thresholds: 100 and 150 mm in 24 h for daily precipitation, and hourly thresholds ranging from 10 to 50 mm in 1 hour by 5 mm. Caillaud et al. (2023) studied the areas with precipitation exceeding 10 mm in 1 hour during days with precipitation accumulation exceeding 100 mm on at least one grid cell of the French Mediterranean area. The aim is to track the convection cells and assess the sub-daily changes expected for future precipitation, using projections of convection permitting climate models. Regarding these different methods, one conclusion is that the precipitation thresholds used in order to define a heavy precipitation event (HPE) as heavy can vary considerably from one region to another, depending on the local meteorology.

In this study, a selection method similar to the one used by Lengfeld et al. (2021) was applied to collect HPEs. The precipitation threshold as well as the minimum area with precipitation and the minimum duration between two events were adapted to the typical HPE that occur on the French Mediterranean coast. The method for the selection of HPEs can be summarized as follows:

1. Collection of time steps with precipitation above the heavy precipitation thresholds over a minimum area;
2. Gathering time steps with heavy precipitation collected for each threshold and definition of the start and end dates of each event;
3. Verification of the temporal independence of the HPE selected.

The first step was to collect time steps with heavy precipitation from the COMEPHORE data over the 2007–2020 period. Three precipitation thresholds were used: 40 mm in 1 h, 65 mm in 3 h and 100 mm in 24 h. They were chosen in consultation with the SMIAGE Maralpin, which is the public entity responsible for hydro-meteorological monitoring over the Alpes-Maritimes department. These three precipitation thresholds were defined in order to study short and intense precipitation events as well as longer ones. Heavy precipitations over 3 h or 24 h were selected using the precipitation accumulation computed over a sliding temporal window, centered on 3 h or 24 h for each COMEPHORE grid cell. The COMEPHORE grid cells that were compared to the precipitation thresholds were those within a 25 km perimeter around coastal catchments, as illustrated by the blue dotted line in Fig. 3. Precipitations were defined as "heavy" if the precipitation threshold is exceeded over at least 25 km^2 (i.e., 25 contiguous grid cells of 1 km^2), with at least one cell being over the studied area shown in red in Fig. 1b. In the case of several disjointed areas with precipitation above the threshold, if the surface of at least one area exceeded the minimum surface area of 25 km^2, the time step was collected. When using the precipitation thresholds on 3 hours or 24 h precipitation accumulations, if the value exceeded the threshold for a time step, all hourly time steps corresponding to the 3-hour or to the 24-hour period used to calculate the precipitation accumulation were collected.

Fig. 3 illustrates a time step collected as part of an HPE: the maximum surface of the area with precipitation above 40 mm in 1 h is greater than 25 km^2 and at least one cell of the area with precipitation above 40 mm in 1 hour is included in a catchment of the study area.

The same time step can be collected using more than one precipitation threshold because it exceeded the 1-hour and 3-hour thresholds, for example. So, the second step consisted in pooling together the time steps collected for each duration and removing duplicated time steps to obtain a single list of time steps tagged as "heavy precipitation". Finally, the consecutive time steps from this single list are gathered, defining the start and the end dates of the HPE as the first and the last time step with heavy precipitation.

The third and final step was to check the temporal independence of the selected HPEs. To be considered temporally independent, an HPE must be at least 24 h apart from the others. The HPEs that are less than 24 hours apart are grouped together.

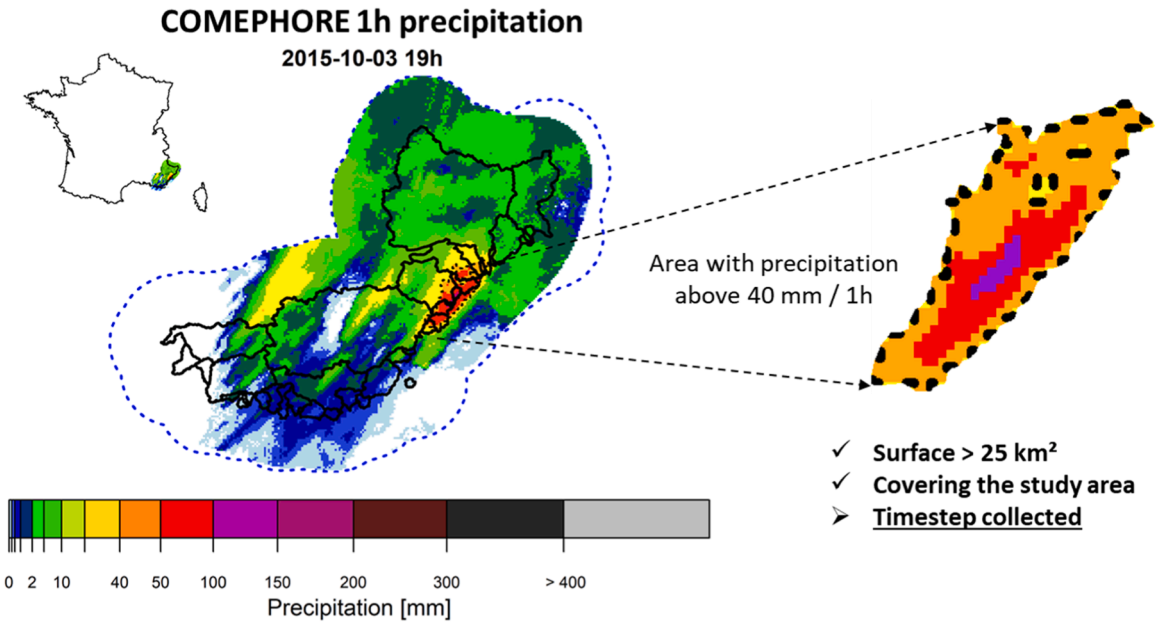

Fig. 3. example of one timestep with heavy precipitation.

Finally, in the database that includes all the HPEs, there are HPEs with precipitation exceeding only one, two or three of the three heavy precipitation thresholds. HPEs lasting more than 1 h do not necessarily have precipitation exceeding the 1-hour heavy precipitation threshold in the first hour, the precipitation accumulation may be exceeding a precipitation threshold in the 3 first hours or the 24 first hours, depending on the threshold used to select each HPE. In addition, HPEs lasting more than 24 hours do not necessarily have precipitation exceeding the 24-hour heavy precipitation threshold in the HPE. It is possible that during these HPEs the precipitation is exceeding only the 1-hour and/or 3-hour thresholds several times leading to an episode lasting more than 24 h in total.

3.2. HPE spatio-temporal characteristics

This section describes the spatial and temporal characteristics that are used to describe the HPEs.

3.2.1. HPE classification

At the end of the selection process, a database of HPEs was generated. These HPEs are classified into two categories:

c1) HPEs that are associated with at least one high flow event (HFE) on a gauged catchment;

c2) HPEs that are not associated with a HFE.

To determine if an HPE is associated with a HFE, the maximum hourly river discharge observed during the HPE duration is compared with the 95 % empirical quantile of the hourly river discharges (noted Q95, computed using hourly river discharges over the period 2007–2020): if the maximum river discharge observed during the HPE is above the 95 % quantile, it is considered as a HFE. Note that, in this study, a HFE means that river discharges were significantly high compared to past observations; it does not mean the river actually overflowed. In addition, one HPE may be associated with (i) none, (ii) one or (iii) more than one HFE, as the HPE may affect several catchments and the catchment areas affected may or may not have reacted to precipitation, or one or more catchment areas may have observed high flows caused by heavy precipitation.

The HPEs collected are also classified using seasons, with spring HPEs being those with a start date in March, April or May, summer HPEs being those with a start date in June, July or August, fall HPEs being those with a start date in September, October or November, and winter HPEs being those with a start date in December, January or February.

3.2.2. Data used to compute characteristics

The characteristics of the HPEs are computed from the COMEPHORE hourly, 3 hours and 24 hours precipitation accumulation grid cells over the studied area (noted hereafter $RR_{grid,\ 1\,h}$; $RR_{grid,\ 3\,h}$; $RR_{grid,\ 24\,h}$, respectively) and COMEPHORE total precipitation accumulated during the duration of the HPE (noted hereafter $RR_{grid,HPE}$). The characteristics of the HPEs that affected the gauged catchment are also computed from the COMEPHORE grid cells covering each catchment area individually (noted hereafter $RR_{catch,1\,h}$; $RR_{catch,3\,h}$; $RR_{catch,24\,h}$, respectively) and by the catchment precipitation time series (noted hereafter P_{catch}). P_{catch} is computed at each hourly time step as the spatial average of the values of the precipitation grid cells intercepting the catchment. The values of the precipitation grid cells are weighted by the surface of the cell inside the catchment area. A catchment may have been affected by lighter precipitation for a few hours just before or after the heavy precipitation. To take this into account and study the entire precipitation event that affected the catchment, the temporal window used to study the catchment precipitation is updated by shifting the start and end dates of the HPE by a few hours until the catchment precipitation is below 0.1 mm. The temporal window can be increased by a maximum of 24 h to not overlap with other HPE. Then, to study the river discharges, the time window defined to study the precipitation is shifted by the rainfall-runoff lag time, in order to take into account the time it takes for the rain to runoff over the catchment and up to the outlet. The rainfall-runoff lag time is computed for each catchment as the time lag that maximizes the cross-correlation between catchment rainfall and river discharges (Ficchì et al., 2016; Astagneau et al., 2021).

3.2.3. Computed characteristics

First, the number of HPEs in each class (c1 or c2 and season) is computed. Then, the area most affected by these episodes is described, looking at:

- the number of times that each COMEPHORE grid cell is affected by heavy rainfall during all the HPEs over the MedEst area. Computed for each COMEPHORE grid cell as described by Equation 1.

  Equation 1: number of times that each COMEPHORE grid cell is affected by heavy rainfall.

$$\sum_{t=1}^{n} \begin{cases} 1, \&if RR_{grid,\ 1h} > 40mm\ in 1hour \\ \quad or RR_{grid,\ 3h} > 65mm\ in 3hour \\ \quad or RR_{grid,\ 24h} > 100mm\ in 24hour \\ 0, \&else \end{cases} \quad [h]$$

  With t being all the hourly time steps during all the HPEs duration and n being the total time steps.

- the total amount of precipitation accumulated during all the HPEs on each cell of the COMEPHORE grid over the MedEst area. Computed for each COMEPHORE grid cell as described by Equation 2.

  Equation 2: total amount of precipitation accumulated during all the HPE.

$$\sum_{t=1}^{n} RR_{grid,\ 1h} \quad [mm]$$

the number of times each catchment has been affected by an HPE. We consider a catchment has been affected by an HPE when there is at least one grid cell over the catchment with rainfall rate above the heavy precipitation threshold on the duration of the event (i.e. at least one grid cell with $RR_{catch,1\ h} > 40$ mm in 1 h, or $RR_{catch,3\ h} > 65$ mm in 3 h, or $RR_{catch,24\ h} > 100$ mm in 24 h).
- how many HPEs are associated with an HFE. We consider a catchment has been affected by an HPE with an HFE when the maximum river discharge associated with the HPE is above the Q95 discharge threshold.

Finally, metrics are calculated in order to describe the spatio-temporal characteristics of each HPE. These metrics are:

- the duration of the HPE;
- the maximum $RR_{grid,1\ h}$, $RR_{grid,3\ h}$, $RR_{grid,24\ h}$ and $RR_{grid,HPE}$ values;
- the total area of the HPE (computed as the number of grid cells with $RR_{grid,1\ h}$ or $RR_{grid,3\ h}$ or $RR_{grid,24\ h}$ above the heavy precipitation threshold on at least one timestep);
- the spatial variability of the precipitation accumulation (computed as the standard deviation of all the $RR_{grid,HPE}$ values). To better illustrate the spatial variability, we also used a relative standard deviation computed as the standard deviation of all the $RR_{grid,HPE}$ values divided by the $RR_{grid,HPE}$ maximum value.

Additional metrics are calculated for each HPE that affected a gauged catchment, and for each gauged catchment impacted, as follows:
- the maximum $RR_{catch,\ 1\ h}$, $RR_{catch,\ 3\ h}$ and $RR_{catch,\ 24\ h}$ values;
- the maximum P_{catch} value on one timestep;
- the sum of P_{catch} over the HPE duration;
- the spatial variability of the $RR_{catch,HPE}$ values;
- the surface of the catchment affected by the HPE.

The precipitation maximum values ($RR_{grid,1\ h}$, $RR_{grid,3\ h}$, $RR_{grid,24\ h}$ and $RR_{catch,\ 1\ h}$, $RR_{catch,\ 3\ h}$ and $RR_{catch,\ 24\ h}$) are computed for each event for all three durations (1 h, 3 h and 24 h) even if they did not exceed the three heavy rainfall threshold of 40 mm in 1 h, 65 mm in 3 h and 100 mm in 24 h.

All the parameters computed to characterize HPEs as well as their definition and the data used to compute them are summarized in Table 1.

4. Results

Based on the COMEPHORE precipitation over 2007–2020, a total of 158 HPEs were selected, totaling 3417 h. Out of the 158 HPEs that affected the gauged catchments, 103 were associated with at least one HFE. The majority of the events exceeded all three precipitation thresholds:

- 30 % of HPEs (47 / 158) have precipitation exceeding the three heavy precipitation thresholds (i.e., $RR_{grid,1\ h} > 40$ mm in 1 h and $RR_{grid,3\ h} > 65$ mm in 3 h and $RR_{grid,24\ h} > 100$ mm in 24 h over an area of at least 25 km^2 over at least one time step). Out of these 47 HPEs, there are 42 HPEs with at least one HFE;

Table 1
parameters computed to compare spatio-temporal characteristics of heavy precipitation events.

Parameter	Definition	Data source
$RR_{grid,1\ h}$ [mm/h] $RR_{grid,3\ h}$ [mm/3 h] $RR_{grid,24\ h}$ [mm/24 h]	Precipitation value from one grid cell over the MedEst area.	COMEPHORE 1 h, 3 h or 24 h precipitation accumulation
$RR_{catch,\ 1\ h}$ [mm/h] $RR_{catch,\ 3\ h}$ [mm/3 h], $RR_{catch,\ 24\ h}$ [mm/24 h]	Precipitation value from one grid cell over the studied catchment.	COMEPHORE 1 h, 3 h or 24 h precipitation accumulation
dt	HPE duration.	
$RR_{grid,HPE}$ [mm/dt]	Precipitation value from one grid cell over the MedEst area.	COMEPHORE precipitation accumulation over the event duration
$RR_{catch,HPE}$ [mm/dt]	Precipitation value from one grid cell over the studied catchment.	COMEPHORE precipitation accumulation over the event duration
P_{catch} [mm/h]	Catchment rainfall. Computed as the weighted mean from the precipitation of all the grid cells intercepting the studied catchment.	COMEPHORE hourly precipitation
Q95	Quantile 95 % computed from the river discharges of the station over the 2007–2020 period.	River discharges from HydroPortail.

- 21 % of HPEs (34 / 158) have precipitation exceeding only the 1-hour heavy precipitation threshold. Out of these 34 HPEs, there are 9 HPE with at least one HFE;

- 3 % of HPEs (5 / 158) have precipitation exceeding only the 3-hour heavy precipitation threshold. Out of these 5 s HPE, there is 1 HPE with at least one HFE;

- 18 % of HPEs (29 / 158) have precipitation exceeding only the 24-hour heavy precipitation threshold. Out of these 29 HPEs, there are 28 HPEs with at least one HFE;

- the remaining episodes have precipitation exceeding two of the three thresholds (20 % of HPEs exceeded the 1-hour and the 3-hour precipitation thresholds but not the 24-hour one, 5 % of HPEs exceeded the 3-hour and the 24-hour precipitation thresholds but not the 1-hour one and 1 % (or 2 HPEs / 158) of all the HPEs exceeded the 1-hour and the 24-hour precipitation thresholds but not the 3-hour one);

- In total, 115 HPEs have precipitation exceeding the 1-hour precipitation threshold (/158 HPEs). These 115 HPEs may have only exceeded the 1-hour threshold, or they may also have exceeded 3-hour or/and the 24-hour thresholds. Out of these 115 HPEs, there are 66 HPEs with at least one HFE.
- In total, 93 HPEs have precipitation exceeding the 3-hour precipitation threshold (/158 HPEs). These 93 HPEs may have only exceeded the 3-hour threshold, or they may also have exceeded the 1-hour or/and the 24-hour thresholds. Out of these 93 HPEs, there are 64 HPEs with at least one HFE.
- In total, 87 HPEs have precipitation exceeding the 24-hour precipitation threshold (/158 HPEs). These HPEs may have only exceeded the 24-hour threshold, or they may also have exceeded the 1-hour or/and the 3-hour thresholds. Out of these 87 HPEs, there are 81 HPEs with at least one HFE.

4.1. Frequency and spatial variability of HPE

To examine the inter-annual and seasonal variability of HPEs, we summarize in Fig. 4 the number of HPEs collected each year and each season. The hatched portion of Fig. 4 illustrates the number of HPEs that caused HFE and the non-hatched portion the number of HPEs represents the areas where no HFE were detected. The number of HPEs collected is greatly variable according to the years and the seasons. Between 5 and 19 HPEs have been collected per year. HPEs are generally more frequent in early summer and autumn (75 % of HPEs), but the distribution of HPEs by season varies from year to year. A large proportion of autumn HPEs were associated with HFEs (out of the 61 HPEs collected in autumn 48 were associated with at least one HFE). Despite a rather large number of HPEs collected in summer (58 HPEs / 158), less than half of these events were associated with HFEs (24 out of 58 summer HPEs). The number of HPEs collected in spring is low compared with other seasons, but these HPEs were often associated with HFEs.

Fig. 5 illustrates the number of catchments impacted (in gray) by each HPE and the number of catchments that experienced a HFE in reaction to the HPE (portion hatched in red). Looking at the number of catchments affected by each HPE, there are very short HPEs

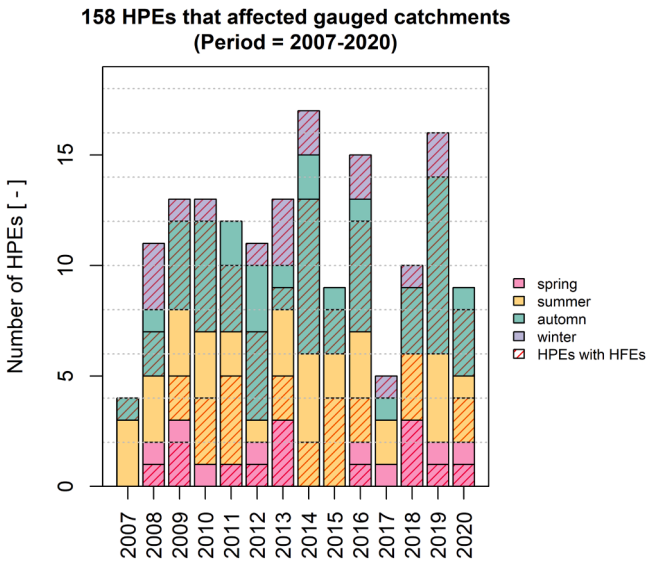

Fig. 4. number of HPEs collected each year and distribution by season, the hatched part shows the portion of HPEs that caused at least one HFE on a gauged catchment.

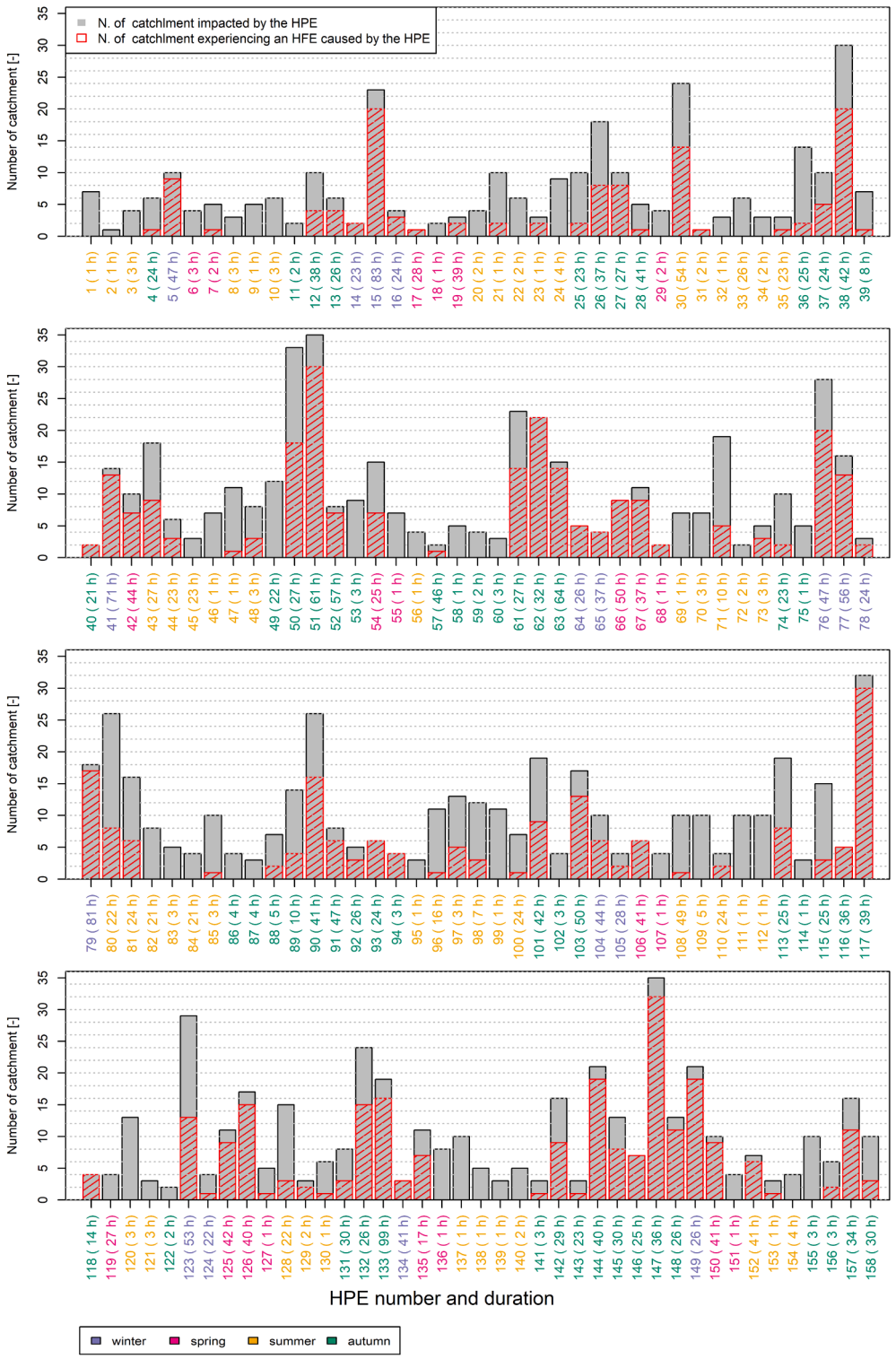

Fig. 5. number of catchment impacted by each HPE (in gray) and number of catchment that experienced an HFE caused by the HPE (portion hatched in red). The event number and duration are given on the x axis. The color of the event number corresponds to the season.

(lasting less than 3 h) that only exceed the 1-hour heavy rainfall threshold affected between 1 and 11 catchments. Short HPEs (lasting less than 6 h) affect between 1 and 13 catchments, while longer HPEs (lasting more than 6 hours) affect between 1 and 35 catchments. The number of HPEs that caused HFEs varies greatly from one to another. Of the 104 HPEs that caused at least one HFE over one

catchment, 16 HPEs caused HFEs over all the catchments affected. The number of catchments affected by these HPEs varies between 1 and 22 (for HPE n°62).

Fig. 6 shows the number of HPEs that affected each gauged catchment (in blue) and the number of events among these that are associated with a HFE (hatched part). The average number of HPEs identified per catchment is 41, and the average number of HPEs with a HFE is 20. The number of times each catchment was affected by a HPE varies from one catchment to another. The catchments most frequently affected by HPEs are naturally the largest ones (the Argens at Roquebrune-sur-Argens, (n°20), the Argens at Arcs (n°17), and the Var at Nice (n°34)), followed by smaller catchments such as the Gapeau at Hyeres (n°12), the Siagne at Pegomas (n°27) or the Loup at Villeneuve-Loubet (n°32). It can also be seen that a small catchment of (the Giscle at Cogolin (n°19)) was affected by more HPE than the average. The Cadière in Marignane catchment (n°2) has experienced the least HPE and all the HPEs selected were associated with HFEs. In general, for small catchments ($S < 100$ km^2), the percentage of HPE associated with HFE is high (77 % on average) compared with larger catchments (54 % on average). The Argens at Roquebrune-sur-Argens catchment (n°20) is most often hit by the HPEs, it has been affected by 113 HPEs (out of the 158 selected).

In order to evaluate if any area was more frequently affected by heavy rainfalls, Fig. 7a shows how many times each COMEPHORE grid cell was associated with an HPE (computed for each COMEPHORE grid cell using Equation 1), while Fig. 7b shows the total amount of precipitation accumulated when considering all the HPEs time steps (computed for each COMEPHORE grid cell using Equation 2). Firstly, Fig. 7a and b show that there is a great spatial variability when looking at the number of HPEs, as well as when considering the precipitation accumulation amounts affecting each cell. Fig. 7a shows that some areas were more frequently impacted by HPEs (dark orange and red colors) than others (green colors). Fig. 7b highlights several particular areas that tend to receive more precipitation (purple and black colors) than others during HPEs (light blue colors). Fig. 7a and b show that the areas most impacted by HPEs seem to be the western part of the Gapeau, the Argens, the Giscle, the Préconil, and the Siagne catchments (these catchments are identified using the arrows with their names). The Esteron and Roya catchments were also often affected. The upstream parts of the Loup and the Cagne catchments clearly stand out in Fig. 7b. The westernmost catchments were the less impacted (Arc, Huveaune, Cadière catchments).

4.2. Surface of gauged catchments impacted by HPE

During each HPE, precipitation could have fully or partially covered the impacted catchments. The surface of gauged catchments affected by heavy precipitation varies greatly from one HPE to another, from 0 % to 100 % (because not all the catchments have been impacted by all the HPEs, some HPEs impacted only one or a few of the catchments over the study area and did not impact others). Fig. 8 shows the surface of the gauged catchments covered by heavy precipitation during each HPE in percentage (only for catchments that have been affected by the HPEs, i.e., when the surface covered is more than 0 %). Values are shown in red for HPEs that are associated with HFEs and in blue for those that are not.

The mean surface covered by heavy precipitation represents 21 % of the total surface of the catchment. The median and mean values of surface covered by heavy rainfall during HPEs with HFEs decrease with the size of the catchment. The median surface area impacted by HPEs with HFEs represents 30 % of the total surface area for small catchments (< 100 km^2), 22 % of medium-sized catchments (≥ 100 km^2 and < 500 km^2) and only 7 % of large catchments (≥ 500 km^2). The mean surface area impacted by HPEs with HFEs represents 42 % of small catchments, 35 % of medium-sized basins and only 18 % of large basins. This may be explained by the fact that larger catchments may experience more frequent downstream HFEs caused by a sub-catchment reaction to heavy precipitation. On the contrary, smaller catchments may experience more frequent HFEs caused by the reaction of the main river and its tributaries while the reaction of only one sub-catchment is not sufficient to cause a HFE. Nevertheless, HFEs were observed when HPEs covered small parts of the catchments and, alternatively, some HPEs that covered a rather large portion of some catchments were not associated with HFEs. For example, 25 % of HPEs without HFE on the Reppe at Ollioules (n°8) and Gapeau at Solliès (n°9) catchments have affected more than 60 % of the total area of these catchments. The Gapeau at Solliès (n°9) catchment clearly stands out looking at Fig. 8 as 25 % of the HPEs affected more than 55 % of the surface area of the catchment and did not generate any HFE, whereas some HPEs that affected less than 20 % of the catchment caused HFEs. This may be explained by the fact that 99 % of catchment n°9 is covered by karstic areas.

4.3. Duration of HPE

Other important characteristics of HPEs are their duration and intensity. These characteristics are presented in the following paragraphs. Fig. 9 illustrates the total and monthly distribution of the duration of the HPEs collected (a and b) as well as the distribution of the duration of HPEs with and without HFEs on gauged catchments (c). Fig. 9a shows that the mean duration of all HPEs is 20 h and that 42 % of HPEs (71/166) last less than 6 hours. Fig. 9b shows that the longest HPEs were those occurring in late autumn and winter, and the shorter ones were those occurring in summer and spring. According to Fig. 9c, the longest HPEs (lasting more than 30 hours) were always associated with at least one HFE, representing 46 (out of 158 that affected gauged catchments) HPEs. Looking at shorter HPEs, 18 of the 71 HPEs lasting less than 6 hours were associated with HFEs.

4.4. Intensity of HPE

The intensity of the HPEs is analyzed from three perspectives. First, we consider the $RR_{grid,\ HPE}$ maximum values and second the $RR_{grid,\ 1\ h}$, $RR_{grid,\ 3\ h}$ and $RR_{grid,\ 24\ h}$ maximum values.

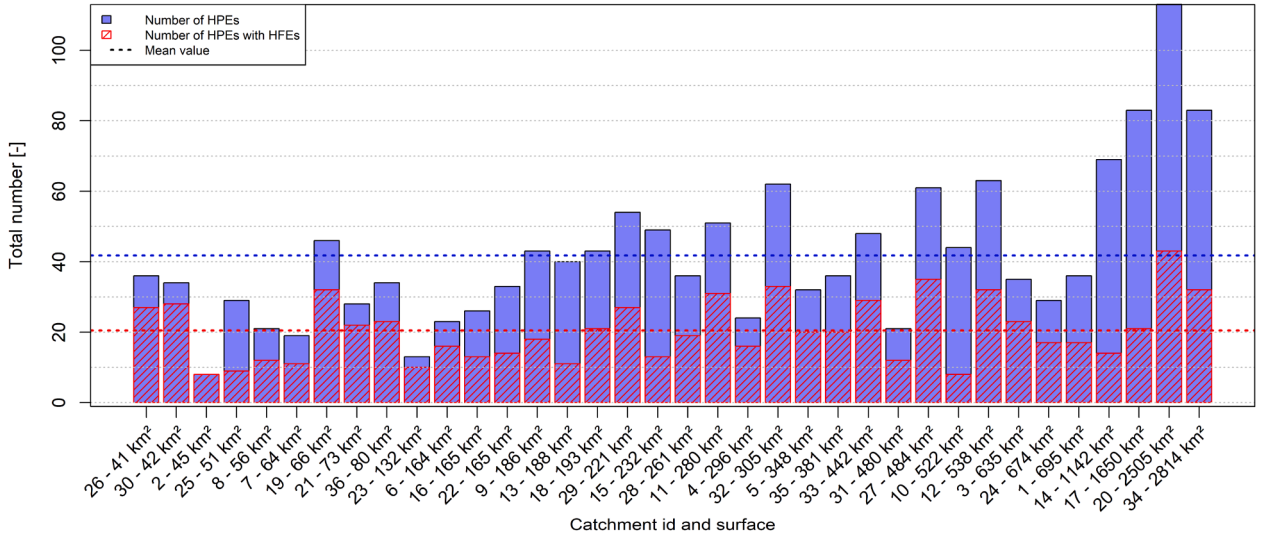

Fig. 6. number of HPEs that affected each catchment (in blue) and total number of HFE observed (hatched in black) for each gauged catchment. The catchments are ordered from the smallest on the left to the largest on the right, and their upstream areas are shown in brackets. The dotted lines indicate the average number when considering all gauged catchments.

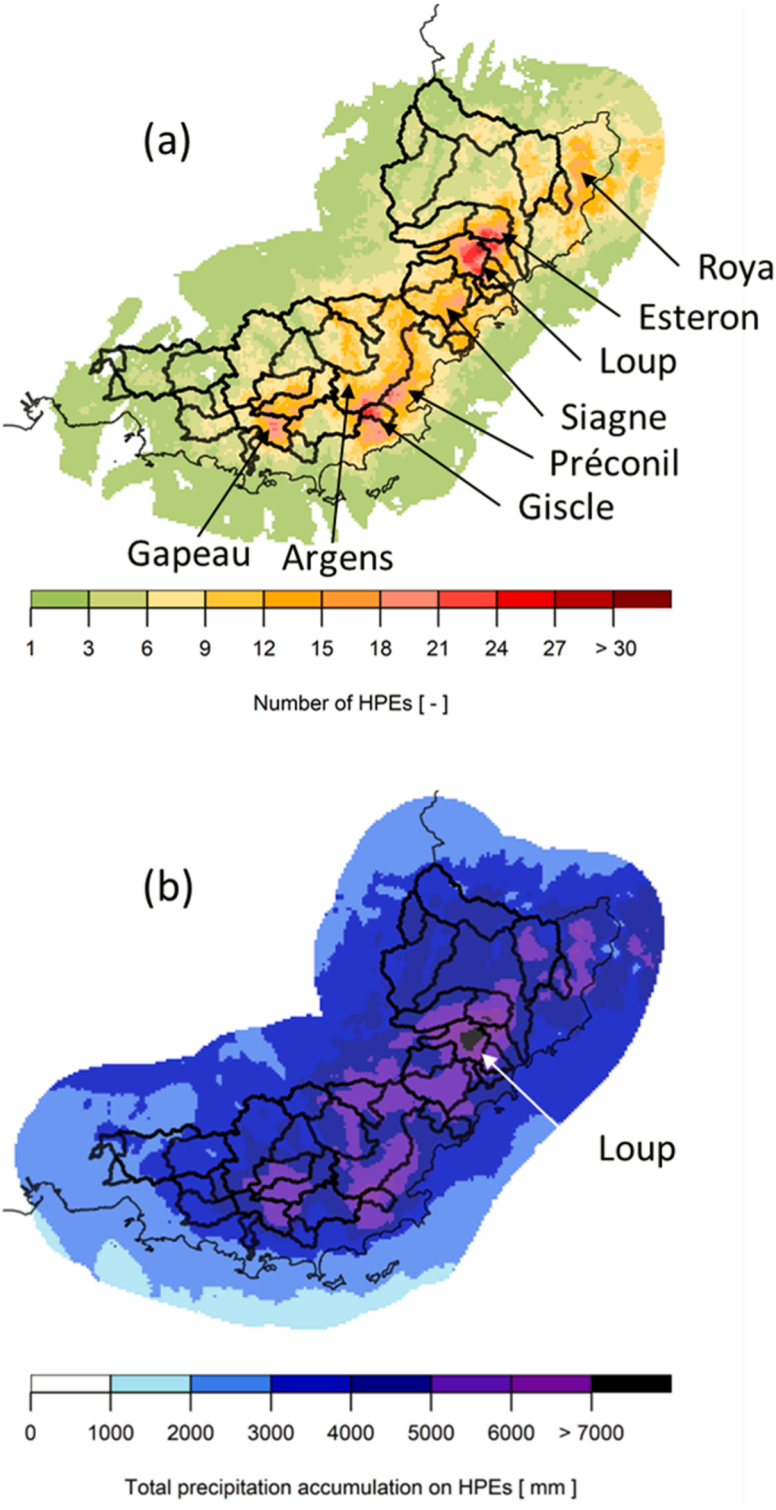

Fig. 7. (a) number of times each cell was associated with an HPE and (b) total amount of precipitation accumulated over the 3417 h of all the 158 HPEs. The black line shows the gauged catchment delineations.

First, Fig. 10 shows the total (Fig. 10a) and monthly (Fig. 10b) distribution of the $RR_{grid,\ HPE}$ maximum values and (c) the $RR_{grid,\ HPE}$ maximum values for HPEs with HFEs in red and HPEs without HFE in blue. The analysis of the $RR_{grid,\ HPE}$ maximum values (Fig. 10b) shows a clear seasonal trend with the highest values observed in autumn and in winter, when the longest HPEs were observed

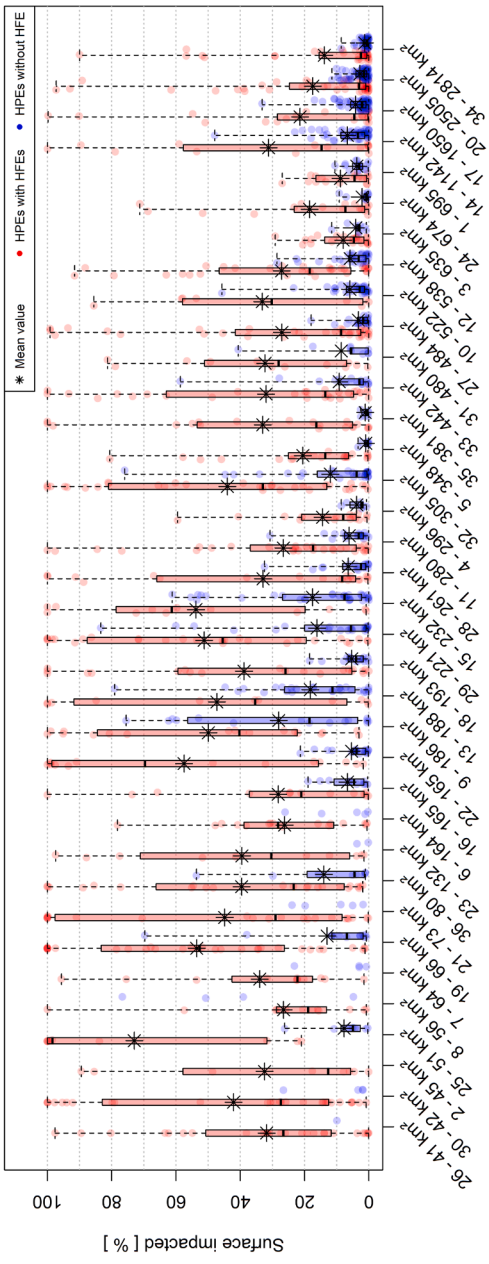

Fig. 8. surface of each catchment impacted by the HPE (in percentage). There are 2 boxplots for each catchment, representing the values for the HPEs with HFEs (in red) and HPEs without HFE (in blue). The catchment ID is shown on the x axis and the catchments are ordered by area. The boxplots are built using the minimum, quantiles 25 %, 50 %, 75 % and the maximum values.

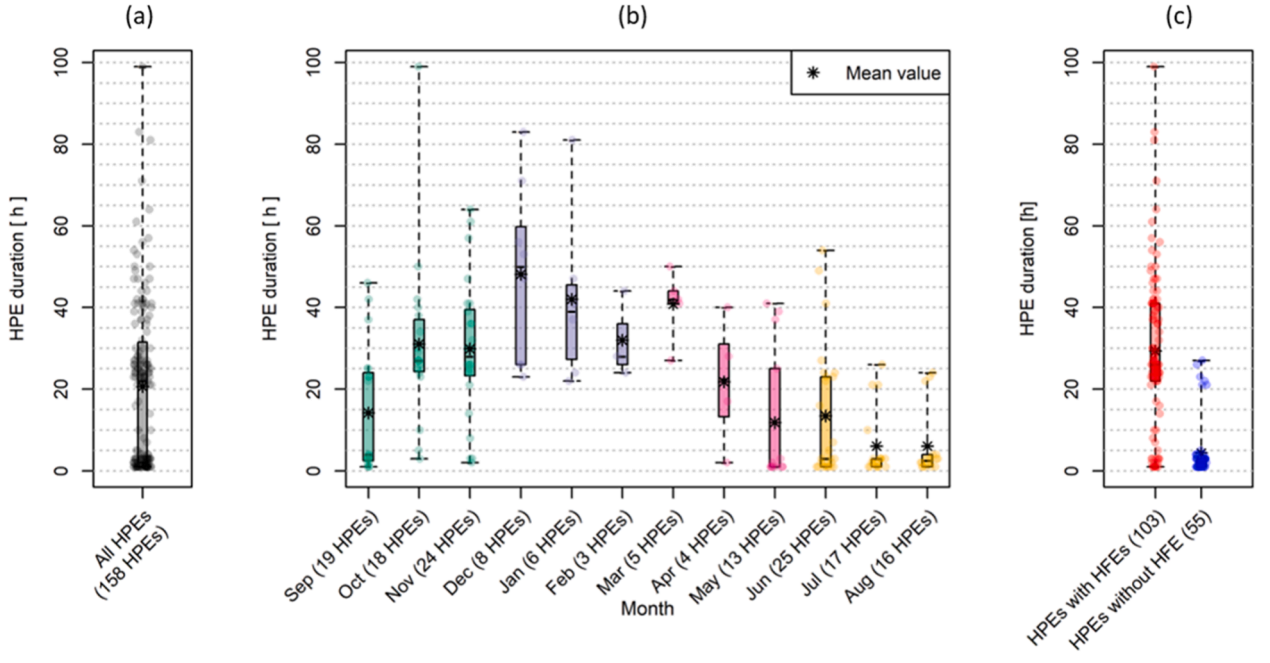

Fig. 9. (a) duration of all HPEs. (b) monthly distribution of the duration of all HPEs. (c) duration of HPEs that did or did not caused HFEs. The boxplots are built using the minimum, quantiles 25 %, 50 %, 75 % and the maximum values.

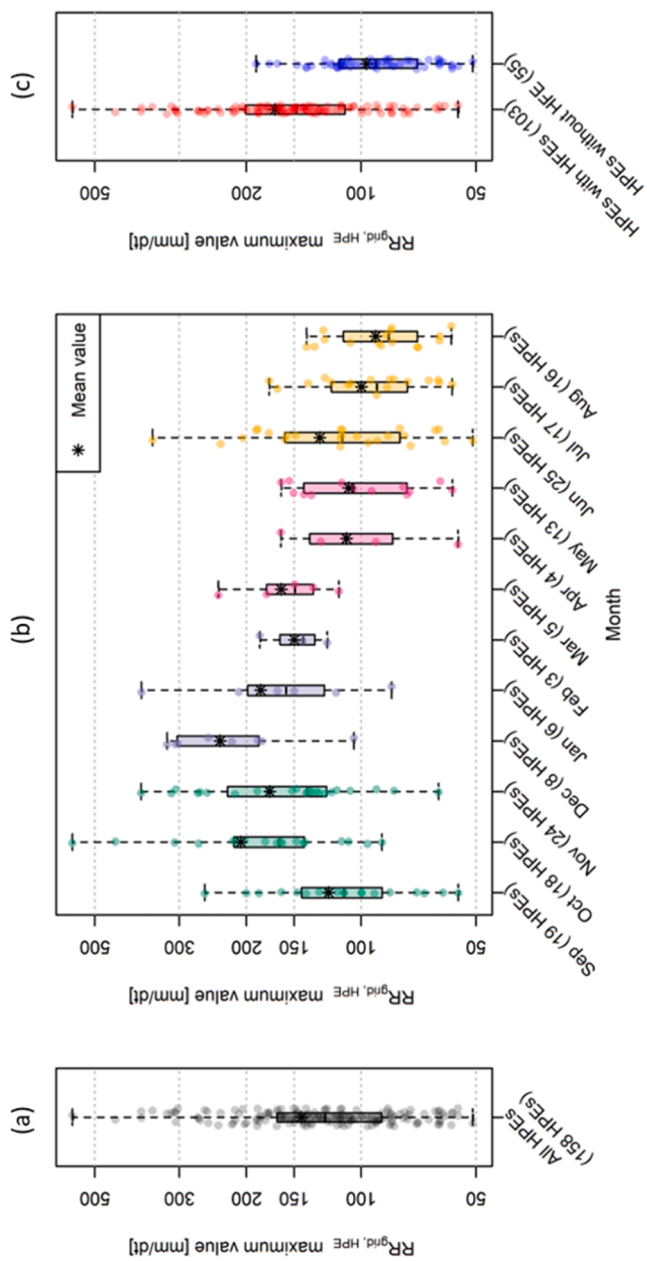

Fig. 10. (a) values of the maximum precipitation accumulation on a grid cell for all HPEs. (b) monthly distribution of maximum point precipitation accumulation for all HPEs. (c) maximum point precipitation accumulation of HPEs that did or did not cause HFEs. The boxplots are built using the minimum, quantiles 25 %, 50 %, 75 % and the maximum values.

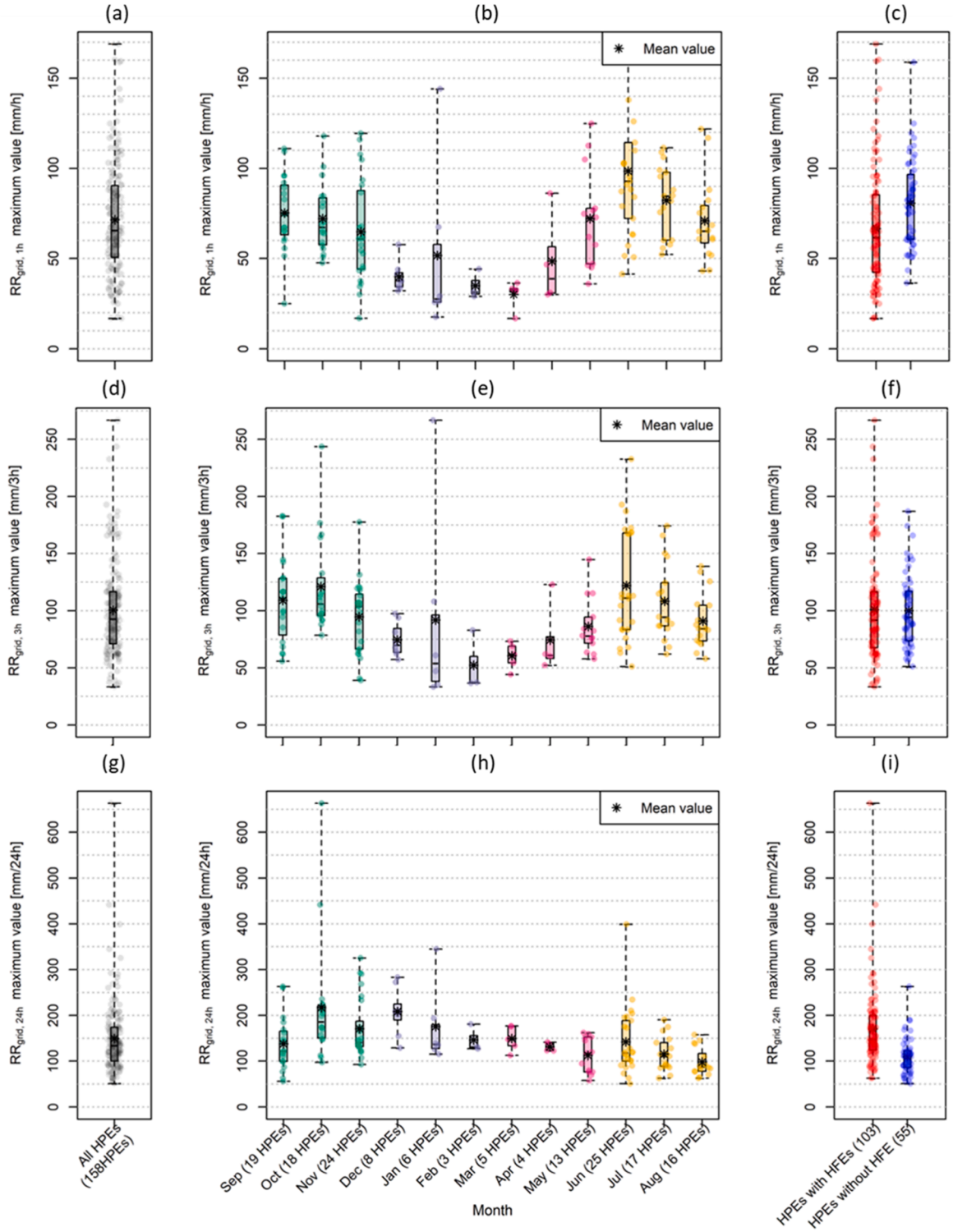

Fig. 11. distribution of maximum point intensities for 1 h (a, b, c), 3 h (d, e, f) and 24 h (g, h, i) for all the HPEs. The first column (a, d, g) shows values for all the HPEs. The second column (b, e, h) shows the monthly distribution of maximum point intensities. The third column (c, f, i) shows values for HPEs with and without HPEs (respectively in red or blue). The boxplots are built using the minimum, quantiles 25 %, 50 %, 75 % and the maximum values.

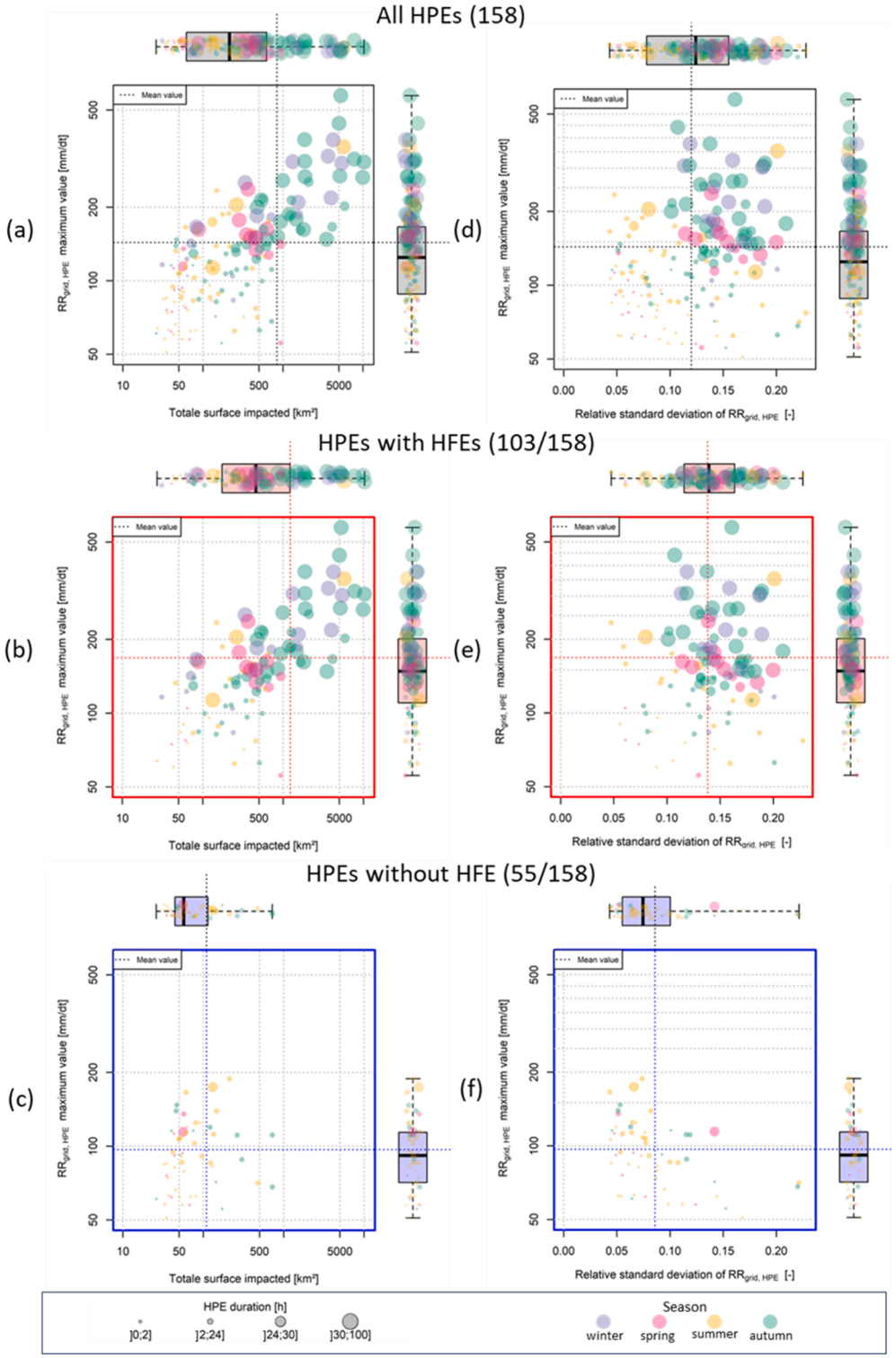

Fig. 12. (a,b,c) the maximum point precipitation accumulation as a function of the surface impacted by heavy precipitation during all the HPEs (d, e, f) the maximum point precipitation accumulation as a function of the standard deviation of the maps of precipitation accumulation. Values for all the HPEs (a, d), for HPEs with a HFE on at least one gauged catchment area (b, e) and for HPEs without HFE on gauged catchments (c, f). The size of the point varies according to the length of the episode: the longer the episode, the larger the dot. The color of the point corresponds to the season (blue dots for winter events, pink dots for spring events, yellow dots for summer events and green dots for autumn events).

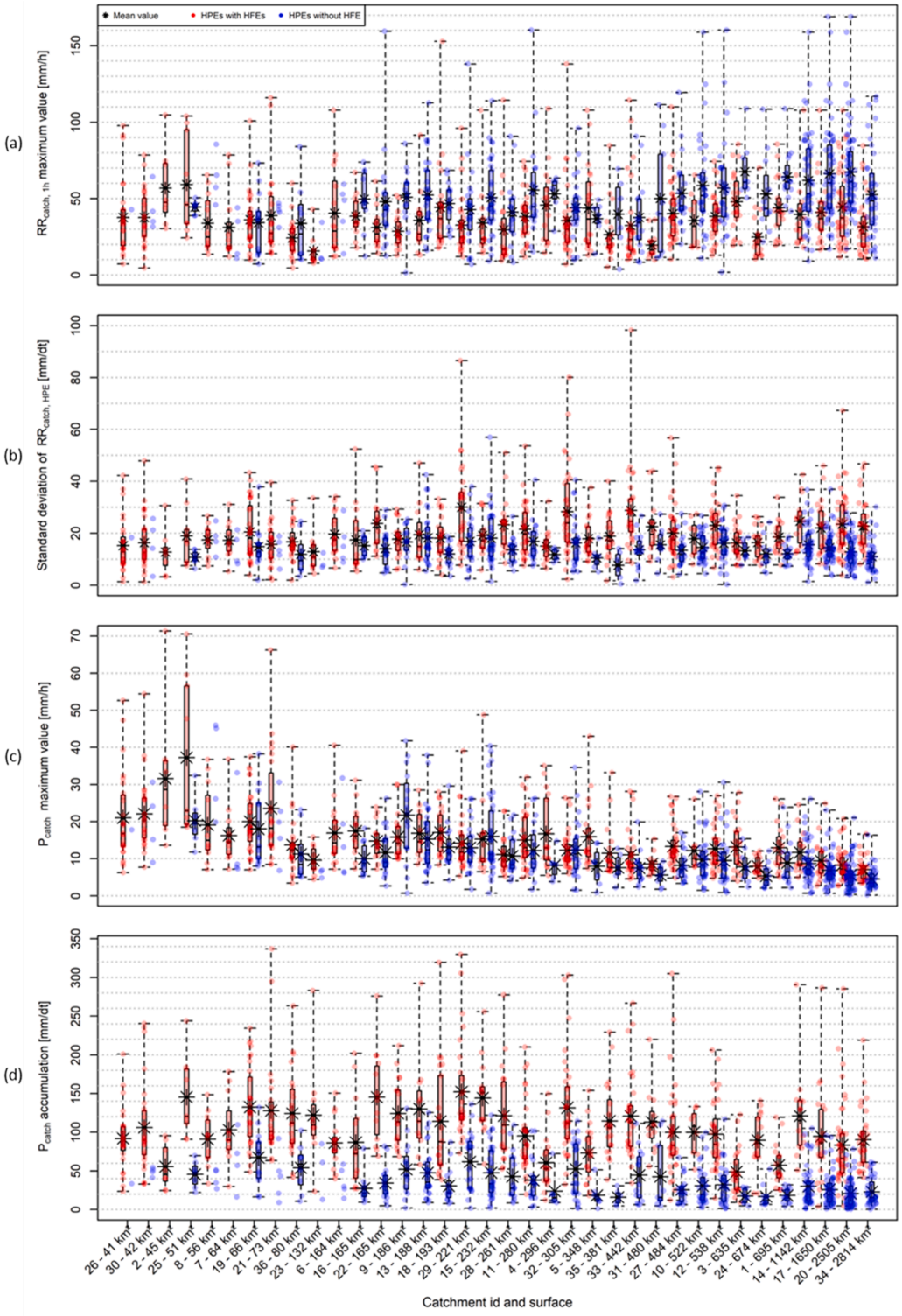

Fig. 13. (a) maximum precipitation intensity on a cell in the catchment for each HPE that affected the catchment area. (b) standard deviation of precipitation accumulation over the catchment. (c) catchment precipitation maximum value. (d) catchment precipitation accumulation over the duration of each HPE that impacted the gauged catchment. There are 2 boxplots for each basin that represent the values for the HPEs with HFEs (in red) and HPEs without HFE (in blue). The catchments ID is shown on the x axis and the catchments are ordered by surface. The boxplots are built using the minimum, quantiles 25 %, 50 %, 75 % and the maximum values.

(Fig. 10b). However, some HPEs occurring at the beginning of the summer were also associated with high values of $RR_{grid,\ HPE}$. Fig. 10c indicates that HPEs with HFEs presents a wide range of values of maximum $RR_{grid,\ HPE}$, even some with small values ($RR_{grid,\ HPE} <$ 100 mm). Fig. 10c shows that the HPEs with maximum $RR_{grid,\ HPE}$ higher than 200 mm were always associated with a HFE. Looking at Fig. 12b (HPEs with HFEs) and Fig. 12c (HPEs without HFE) shows that HPEs with maximum point intensity values between 100 and 200 mm/dt and with HFEs (Fig. 12b) tend to be long HPEs (duration > 24 h) but there are also some shorter HPEs (fewer), and there are also few HPEs lasting more than 24 h without HFE (Fig. 12c). Furthermore, Fig. 12b and Fig. 12c show that there are short HPEs (duration < 24 h) with similar maximum point intensity values (between 50 and 100 mm/dt) but with HFEs and some without HFE.

Second, Fig. 11 shows the total (Fig. 11a, d, g) and monthly (Fig. 11b, e, h) distribution of the $RR_{grid,\ 1\ h}$, $RR_{grid,\ 3\ h}$ and $RR_{grid,\ 24\ h}$ maximum values. The third column of Fig. 11 illustrates the distribution values for HPEs with HFEs (in red) and HPEs without HFE (in blue). The first row (Fig. 11a, b, c) shows the $RR_{grid,\ 1\ h\ values}$, the second row shows $RR_{grid,\ 3\ h}$ maximum values (Fig. 11d, e, f), and the third row shows the $RR_{grid,\ 24\ h}$ maximum values (Fig. 11 g,h, i). The maximum values are computed for each event for all three durations (1 hour, 3 hours and 24 h) even if they did not exceed the three heavy rainfall thresholds of 40 mm in 1 h, 65 mm in 3 h and 100 mm in 24 h.

Fig. 11b shows that HPEs that were observed in early summer (in June) were the most intense ones over 1 hour (highest values of $RR_{grid,\ 1\ h}$ maximum values). However, some winter and autumn HPE also had hourly intense precipitation. Looking at $RR_{grid,\ 3\ h}$ (Fig. 11e), the maximum values are also observed in early summer or autumn, and values are similar for HPEs occurring in summer and autumn. The lowest $RR_{grid,\ 1\ h}$ and $RR_{grid,\ 3\ h}$ maximum values were observed during winter and spring. At 24 hours (Fig. 11 f), the $RR_{grid,\ 24\ h}$ maximum values seem to be higher during the HPEs observed in autumn and winter, with lowest values in spring and summer.

Fig. 11 g, h, i, show that HPEs with HFEs present a wide range of maximum point intensities. Fig. 11i shows that all HPEs with rainfall intensities locally exceeding 270 mm in 24 h were systematically associated with HFEs.

Fig. 11c and Fig. 11 f show HPEs without HFE with higher intensities than for HPEs with HFEs. This is explained by the fact that in the HPE database there are many long episodes (dt > 24 h) with significant 24-hour precipitation accumulation that caused HFEs. But during these long HPEs that caused HFEs, the hourly and 3-hour precipitation accumulations are not very high, which pulls the distributions in Fig. 11c and f downward.

4.5. Summary of the intensity-duration-area of HPE

The characteristics related to duration, intensity and impacted surface of all the HPEs are summarized in Fig. 12a. These characteristics are also compared for HPEs with and without HFEs (Fig. 12b and c). The colors of the points on Fig. 12 correspond to the seasons of the year. The size of the points on Fig. 12 is a function of the HPE duration.

The surface of the MedEst area impacted by heavy precipitation and the precipitation intensity are loosely related. HPEs that affected the largest areas were almost exclusively observed in autumn and winter (represented by the green and blue dots in the top right quarter of Fig. 12a). There were also some winter, summer and autumn HPEs that impacted rather small surfaces with high precipitation accumulations (dots in the top left section of Fig. 12. The HPEs with long durations (> 30 h) were all associated with a HFE. These long events are also associated with a wide range of $RR_{grid,\ HPE}$ maximum values, ranging from 113 mm in 40 h to 572 mm in 34 h. These long episodes impacted surfaces ranging from 71 km^2 to more than 10,000 km^2. Fig. 12b shows that HPEs of short duration (< 24 h) with HFEs have affected the larger catchment areas of the study region, compared to HPEs with the same duration and intensity that were not associated with a HFE. Fig. 12c shows that most of the HPEs with short duration are HPEs without HFE. These short duration HPEs without HFE were still associated with a wide range of precipitation intensities with $RR_{grid,\ HPE}$ maximum values ranging from 60 mm to 200 mm in less than 24 h. They impacted shorter surfaces than HPEs with HFEs, the median impacted surface is around 90 km^2.

4.6. Spatial variability of HPE

Another HPE characteristic of interest is the spatial variability. To analyze it, we computed, for each HPE, the standard deviation of the precipitation accumulated over its duration, considering all grid cells inside the studied area ($RR_{grid,\ HPE}$).To better illustrate the spatial variability of HPEs, Fig. 12 shows the $RR_{grid,\ HPE}$ maximum value as a function of the relative standard deviation of $RR_{grid,\ HPE}$ for each HPE. The relative standard deviation is computed as the standard deviation of $RR_{grid,\ HPE}$ divided by the $RR_{grid,\ HPE}$ maximum value. The points are more scattered for the small $RR_{grid,\ HPE}$ maximum values, which could indicate that the HPEs with small precipitation accumulations (thus heavy precipitation over shorter duration) are more heterogeneous in terms of spatial variability, whereas HPEs with higher precipitation accumulations have more similar spatial variabilities (points are closer together on the upper part of Fig. 12d). Finally, when comparing Fig. 12e and Fig. 12 f, we can see that HPEs with HFEs (Fig. 12e) displays higher spatial variability too.

4.7. Intensity and spatial variability of HPE at the catchment scale

Finally, to describe the precipitation intensity and spatial variability over the catchments during the HPEs, precipitation is studied at the grid cell (only looking at cells in the catchment area studied, $RR_{catch,\ 1\ h}$ and $RR_{catch,HPE}$) and at the catchment scale (P_{catch}).

Fig. 13a illustrates the $RR_{catch,\ 1\ h}$ maximum value for each HPE. Values are compared for HPEs with or without HFEs on each catchment (shown respectively in red and blue). The results show that the $RR_{catch,\ 1\ h}$ maximum values do not have a direct influence

on the occurrence of HFE. For all the catchments, there were HPEs that caused a HFE even though the $RR_{catch,\ 1\ h}$ was not very high, and, alternatively, there were HPEs with high $RR_{catch,\ 1\ h}$ not associated with HFE. Fig. 13b shows the standard deviation of $RR_{catch,\ HPE}$ for HPEs that impacted the catchment. It shows that HPEs the most varying in space were often associated with HFEs. However, there were some HPEs with HFEs with low values of standard deviation. Alternatively, there were some HPEs without HFE with high values of standard deviation. More generally, the median standard deviation is lower for HPEs without HFE than for HPEs with HFEs.

Looking at maximum values of P_{catch} for each catchment for HPEs with or without HFEs (Fig. 13c), the results show that the highest values did not necessarily lead to a HFEs. Values of the same magnitude were associated with both HPEs with HFEs and HPEs without HFE. Fig. 13d shows the P_{catch} accumulation observed during each HPE with or without HFE. For all the catchments, HPEs that generated the highest P_{catch} accumulation were clearly associated with HFEs. All the HPEs for which the P_{catch} accumulation exceeded 150 mm over the HPE duration were associated with a HFE. However, for most catchments, there were HPEs with HFEs and HPEs without HFE with similar values of P_{catch} accumulation (for instance, looking at catchment n°19, some HPEs with catchment precipitation accumulation up to 80 mm are associated with HFEs -red points- and others are not – blue points). The difference between HPEs with or without HFE for the same catchment precipitation accumulation value is most probably the number of time steps with precipitation. It may also be influenced by the portion of the catchment impacted by heavy precipitation, the soil moisture and whether the river discharge was already high before the episode.

5. Discussion

This study focused on the hydro-meteorological characteristics of Heavy Precipitation Events (HPEs) over the southeastern part of the French Mediterranean coastal area (MedEst area). This study is based on a HPE database computed from the COMEPHORE precipitation estimates during the 2007–2020 period.

The results obtained allowed us to answer some key questions for storm and flood risk management in the area, as shown below.

1. When (which season) do HPE more often occur in the MedEst area?

Our study shows that the number of HPEs collected is rather variable according to the years and the seasons, but HPEs are more frequent in early summer and autumn. A large proportion of autumn HPEs are associated with high flow events (HFEs). This is overall in agreement with other studies (Nuissier et al., 2011; Ricard et al., 2012) and complements other works giving HPEs intensities and accumulation values observed during HPE according to the season. HPEs with maximum point precipitation accumulation higher than 200 mm are always associated with a HFE. HPEs observed in early summer (in June) are the most intense over 1 h, however some winter and autumn HPEs have also hourly intense precipitation. At 24 h, the maximum point precipitation values are higher during HPEs observed in autumn and winter.

2. Where do HPE more often occur?

This study shows that locally some areas are most often impacted by HPEs the western part of the Gapeau catchment, the Argens, the Giscle, the Préconil, the Siagne, the Loup, the Cagne, the Esteron and the Roya catchments. The upstream part of the Loup and the Cagne catchments have received more precipitation cumulated during all the HPEs than other areas.

3. How long lasts the HPE?

The mean duration of all the HPEs is 20 hours, and 42 % of HPEs (66/158) last less than 6 hours. There were more short episodes than very long episodes (HPEs lasting more than 30 hours accounted for 40 HPEs / 158, i.e., 25 % of all HPEs). However, all the very long episodes (40 HPEs/40 lasting more than 30 h) caused at least one HFE, while only 18 short HPEs (/66 HPEs lasting less than 6 h) caused at least 1 HFE.

4. At the catchment scale, are there some common characteristics to the HPE with HFE?

The results show that the catchment precipitation accumulation is clearly linked to the HFE generation. Regardless of the catchment, all the HPEs for which the accumulation of catchment precipitation exceeded 150 mm over the HPE duration were associated with HFEs. The maximum point rainfall, the spatial variability of precipitation over the catchment and the maximum catchment rainfall values have been presented for all HPEs that affected the gauged catchments. At first sight, it is difficult to differentiate between HPEs with and without HFEs, simply by looking at the spatial variability or the maximum point intensity of the precipitation. The difference between them is most probably the number of time steps with precipitation, the surface impacted by heavy precipitation. HFE generation may also be influenced by soil moisture and whether the river discharge was already high before the episode.

Some limitations of the study can also be mentioned. The results illustrated here are highly dependent on:

1. the choice of studied area and the precipitation thresholds chosen to collect HPE;
2. the data available (hourly precipitation data and river discharges only on gauged outlets).

The hourly precipitation data may be limiting when looking at convective precipitation. In the study area, precipitation can be heavy on shorter periods of less than 1 hour.

Moreover, it is possible that some actual HPEs have been missed in the analysis because of wrong precipitation estimates in the COMEPHORE data. The quality of this database has improved over time with the incorporation of new radars and rain gauges data, but it still does not take into account altitudes to correct the orographic precipitation estimates (Caillaud et al., 2021). Each COMEPHORE precipitation hourly grid is associated with a grid containing the uncertainties linked with the precipitation estimates. A study of the values of the uncertainties on the grid cells in the study area and on the HPE time steps was carried out. Fig. 14a illustrates the mean uncertainty as a function of mean precipitation over the 5 grid cells with maximum precipitation accumulation. Fig. 14b illustrates mean uncertainty as a function of mean precipitation over the 5 grid cells with maximum uncertainty accumulation for each HPE. Most

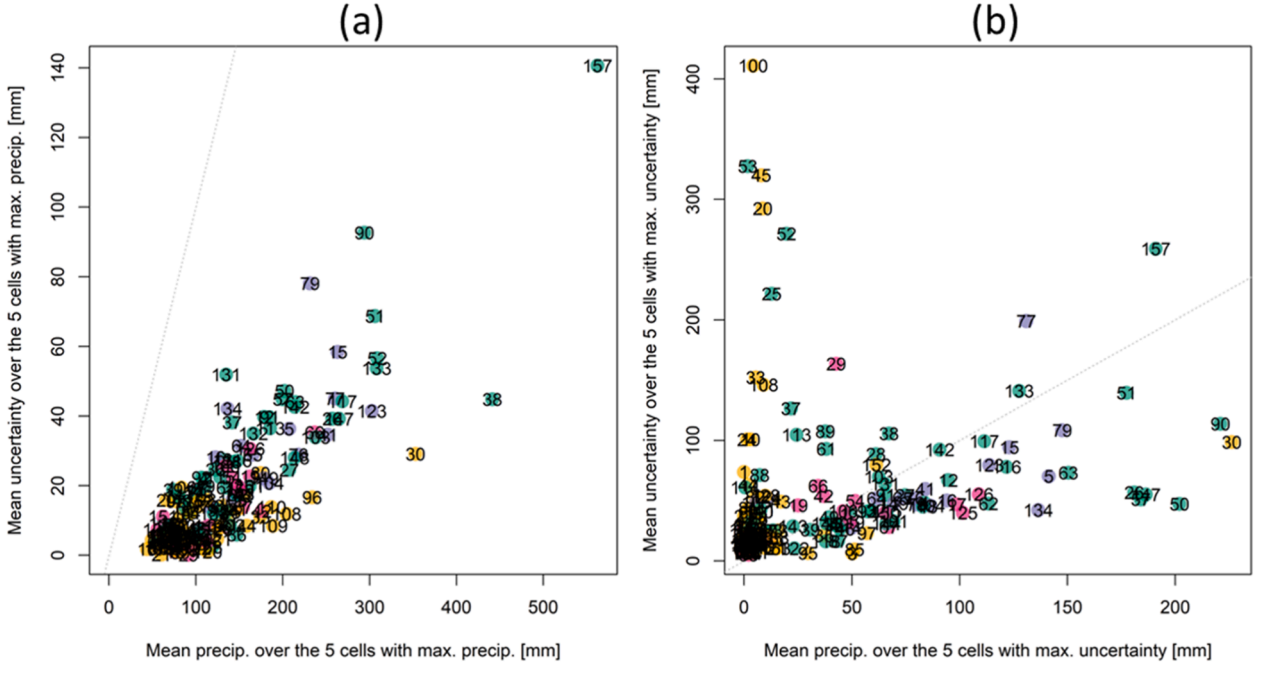

Fig. 14. (a) mean uncertainty as a function of mean precipitation over the 5 grid cells with maximum precipitation accumulation and (b) mean uncertainty as a function of mean precipitation over the 5 grid cells with maximum uncertainty accumulation.

of the HPEs grid cells are associated with pretty small uncertainty values (quantiles 75 % values are below 5 mm/h for all the HPEs), but the maximum values of uncertainty are very high for some HPEs (4 HPEs have maximum uncertainty values above 200 mm/h). Uncertainty seems to increase with rainfall accumulation, as shown on Fig. 14a. The uncertainties are very high on grid cells with high precipitation accumulation for some HPEs (this is the case for HPE n°157, 90 and 79, as shown on Fig. 14a). There are also some HPEs with high uncertainties on grid cells where the cumulative rainfall is very low (this is particularly the case for HPE n°100, 53, 45, 20, 52 and 25, as shown on Fig. 14b). Looking at uncertainty values over HPEs sorted by date, it shows no apparent trend in uncertainty over time.

Furthermore, as the study is based on the COMEPHORE precipitation estimates during the 2007–2020 period (14 years), this study needs to be completed to provide more robust results from a climatological point of view (which requires at least 30 years of data).

Finally, missing discharge data can also lead to an underestimation of the number of HPEs with HFEs.

6. Conclusion

The aim of this study was to make a throughout analysis of the spatial and temporal characteristics of heavy precipitation events (HPEs) that have impacted the gauged catchments of the eastern part of the French Mediterranean coastal area (MedEst area) during the last decade (2007–2020). It focused on identifying common characteristics to these heavy precipitation events and distinguished characteristics for those precipitation events that were associated with high flow events (HFEs) in the gauged catchment areas located in the study area.

We took advantage of the radar/rain-gauge COMEPHORE spatial precipitation estimates over the period 2007–2020 to propose and apply a spatial selection method for heavy precipitation events. The selection method focused on collecting all hourly time steps where the precipitation had exceeded 40 mm in one hour, 65 mm in three hours, or 100 mm in 24 h, and this on at least 25 km^2 (equivalent to 25 contiguous grid cells of the COMEPHORE database). These three rainfall intensity thresholds were chosen after discussing with the local stakeholders responsible for hydro-meteorological monitoring over the Alpes-Maritimes department in France, in order to take account of the local climate.

The spatial and temporal characteristics of the heavy rainfall events were computed from the COMEPHORE gridded data (point precipitation) over the entire studied area, but also on specific gauged catchments at the catchment scale (spatially averaged precipitation). A total of 158 heavy precipitation events have been collected. The seasonal and duration analysis showed that the mean duration is 20 hours and longer episodes are observed during winter and autumn, shorter episodes are observed during summer. The intensity analysis showed that HPE that are observed during summer and spring are the most intense ones over 1 hour and 3 hours accumulation. However, some winter and autumn HPE also have hourly intense precipitation. The mean surface impacted by HPE were 800 km^2.

Heavy precipitation events (HPEs) were classified into two groups as we were interested in comparing the spatial and temporal characteristics of heavy precipitation events that generated high flow events (HFEs) on at least one gauged catchment and the ones that did not and identify some common characteristics of HPEs with HFEs. In order to determine if an HPE was associated with a HFE, the river discharges of the catchments impacted by heavy precipitation were considered. If the maximum river discharge was higher than the 95 % quantile of the hourly river discharges, then we considered that the HPE was associated with a HFE. If the maximum river discharge of one or more than one station exceeded the threshold during the HPE duration, then we considered that the HPE was associated with at least one HFE. For each of these events the following conclusions could be drawn:

c1) HPEs with HFEs: of the 158 HPEs that affected gauged catchments 103 were associated with at least one HFE looking at discharge data at the gauged catchment outlets. The analysis of their duration showed that their mean duration was 30 hours and all the HPEs that lasted more than 30 h are associated with HFEs. The analysis of their intensity showed that all HPEs with catchment rainfall accumulation exceeding 150 mm over their duration are associated with HFEs. The mean surface impacted by HPEs that caused HFE was 1220 km^2.

c2) HPEs without HFE: of the 158 HPEs that affected gauged catchments 53 were not associated with any HFE at the gauged catchment outlets. The analysis of their duration showed that their mean duration was 4 hours, but there are some longer episodes (there are 6 HPE lasting between 21 and 27 h) that are not associated with HFE as well. The analysis of their catchment rainfall accumulation showed that the mean was 35 mm and the maximum was 140 mm over their duration. The mean surface impacted by HPEs that did not cause HFE was 110 km^2.

These spatial and temporal analyses of the characteristics of HPEs that affected the MedEst area during the last decade are key results that allowed us to answer some questions that will support local stakeholders in charge of river monitoring and flood risk alert in the area.

Position, direction and velocities of HPEs have not been studied in this paper but we know some tracking algorithms exist and have been applied by Caillaud et al. (2021) for instance. To go further, we could use a tracking algorithms in order to identify which particular pathways are followed by HPEs or if HPEs that affected the MedEst area are rather stationary or very movable. In addition, the study of HPEs on ungauged catchments may be improved using a damage database to identify HPEs that actually caused flooding (here by flooding we mean an overflowing of the river). Many databases have been built based on flood consequences (human losses and damages) in the past years (Llasat et al., 2010; Vinet et al., 2012; Gaume et al., 2016; Saint-Martin et al., 2018), but they do not contain enough events over our study area in order to draw conclusions regarding precipitation characteristics associated to the flooding events on the study area. In addition, the geology, karstic areas and geomorphology of the catchments undoubtedly also influence the hydrology and the response of the catchments to precipitation. This has been little or not studied at all in this work and it would be interesting to look into it in further research. Finally, in order to improve our knowledge of key drivers for flooding, all the

characteristics (spatial and temporal characteristics of precipitation and geomorphology of catchments) must be studied compared with each other. To achieve this, additional work should be carried out using tools such as classification algorithms or machine learning algorithms.

Declaration of Competing Interest

The authors declare that they have no known competing financial interests or personal relationships that could have appeared to influence the work reported in this paper.

Data availability

Data will be made available on request.

Acknowledgments

The authors would like to thank Météo-France (https://www.data.gouv.fr/en/organizations/meteo-france/, last access: 26/04/2023) and the SCHAPI (https://hydro.eaufrance. fr/, last access: 02/08/2024) for providing the COMEPHORE meteorological database and the streamflow series. We would like to thank Cécile Caillaud for the exchanges we had on heavy precipitation events and COMEPHORE database, and Olivier Laurantin for the clarifications he provided on the COMEPHORE database calculation.

Finally, we thank the two anonymous reviewers for their comments that improved the paper.

AuthorAgreement

The authors declare that they have seen and approved the final version of the manuscript being submitted. They warrant that the article is the authors' original work, hasn't received prior publication and isn't under consideration for publication elsewhere

Appendix 1. Gauged catchments description

The coordinates of the outlet are given in Lambert 93 (ESPG 2154).

ID	Code HYDRO3	Catchment name	Location of the outlet [m]		Area [km^2]
			X_L93	Y_L93	
1	Y412202002	Arc@Berre_l_Etang	874112,5	6269112,5	692
2	Y422561001	Cadiere@Marignane	878762,5	6259212,5	71
3	Y412204001	Arc@Aix	887112,5	6271362,5	635
4	Y402201001	Arc@Meyreuil	903362,5	6270112,5	296
5	Y442404001	Huveaune@Aubagne	907612,5	6246712,5	375
6	Y441403001	Huveaune@Roquevaire	911262,5	6253662,5	165
7	Y441401501	Huveaune@ST_Zacharie	918862,5	6257212,5	56
8	Y451542001	Reppe@Ollioules	930812,5	6229162,5	89
9	Y503201001	Argens@Chateauvert	944812,5	6271462,5	507
10	Y460402001	Gapeau@Sollies	947062,5	6237362,5	187
11	Y461502001	Real_Martin@Crau	953062,5	6236912,5	282
12	Y462401001	Gapeau@Hyeres	956312,5	6232662,5	534
13	Y510501001	Caramy@Vins	956962,5	6265362,5	202
14	Y511201001	Argens@Carces	958612,5	6269562,5	1144
15	Y510661001	Issole@Cabasse	960912,5	6265812,5	235
16	Y511502002	Bresque@Salernes	961062,5	6279112,5	168
17	Y520201001	Argens@Arcs	981062,5	6267012,5	1656
18	Y523501001	Nartuby@Trans-en-Provence	981662,5	6273562,5	195
19	Y542401001	Giscle@Cogolin	987062,5	6246112,5	66
20	Y531201001	Argens@Roquebrune_sur_Argens	994112,5	6267962,5	2512
21	Y532501001	Reyran@Frejus	1002912,5	6271112,5	73
22	Y600203001	Var@Villeneuve_d_Entraunes	1003212,5	6343162,5	132
23	Y551404001	Siagne@Callian	1003462,5	6292062,5	165
24	Y604201001	Var@Entrevaux	1005812,5	6324062,5	674
25	Y550541001	Agay@St_Raphael	1011612,5	6268012,5	48
26	Y553541001	Mourachonne@Pegomas	1017212,5	6284762,5	43
27	Y553403001	Siagne@Pegomas	1017312,5	6284412,5	490
28	Y642401001	Esteron@Sigale	1018012,5	6315312,5	262
29	Y561501001	Loup@Tourettes_s_Loup	1023112,5	6296962,5	206

(*continued on next page*)

(*continued*)

ID	Code HYDRO3	Catchment name	Location of the outlet [m]		Area [km^2]
			X_L93	Y_L93	
30	Y622401001	Tinee@St_Sauveur	1028612,5	6340262,5	480
31	Y560521001	Brague@Biot	1030512,5	6289212,5	42
32	Y561503001	Loup@Villeneuve_Moulin	1033562,5	6292112,5	289
33	Y643401001	Esteron@Broc	1034112,5	6314062,5	441
34	Y644201001	Var@Nice	1038612,5	6294012,5	2812
35	Y633404001	Vesubie@Utelle	1039962,5	6317962,5	382
36	Y663501001	Bevera@Sospel	1057512,5	6318862,5	81

References

Armon, M., Marra, F., Enzel, Y., Rostkier-Edelstein, D., Morin, E., 2020. Radar-based characterisation of heavy precipitation in the eastern Mediterranean and its representation in a convection-permitting model. Hydrol. Earth Syst. Sci. *24* (3), 1227–1249. https://doi.org/10.5194/hess-24-1227-2020.

Astagneau, P.C., Bourgin, F., Andréassian, V., Perrin, C., 2021. When does a parsimonious model fail to simulate floods? Learning from the seasonality of model bias. Hydrol. Sci. J. *0* (ja). https://doi.org/10.1080/02626667.2021.1923720.

Berne, A., Delrieu, G., Boudevillain, B., 2009. Variability of the spatial structure of intense Mediterranean precipitation. Adv. Water Resour. *32* (7), 1031–1042. https://doi.org/10.1016/j.advwatres.2008.11.008.

Blanchet, J., Molinié, G., Touati, J., 2016. Spatial analysis of trend in extreme daily rainfall in southern France. Clim. Dyn. 1–14. https://doi.org/10.1007/s00382-016-3122-7.

Boudevillain, B., Argence, S., Claud, C., Ducrocq, V., Joly, B., Joly, A., Lambert, D., Nuissier, O., Plu, M., Ricard, D., Arbogast, P., Berne, A., Chaboureau, J.-P., Chapon, B., Crepin, F., Delrieu, G., Doerflinger, E., Funatsu, B.M., Kirstetter, P.-E., Walpersdorf, A., 2009. Projet Cyprim, partie I: Cyclogenèses et précipitations intenses en région méditerranéenne: origines et caractéristiques. La MétéOrol. *8* (66), 18. https://doi.org/10.4267/2042/28828.

Boudou, M., Lang, M., Vinet, F., Cœur, D., 2016. Comparative hazard analysis of processes leading to remarkable flash floods (France, 1930–1999). J. Hydrol. *541*, 533–552. https://doi.org/10.1016/j.jhydrol.2016.05.032.

Breugem, A.J., Wesseling, J.G., Oostindie, K., Ritsema, C.J., 2020. Meteorological aspects of heavy precipitation in relation to floods – an overview. Earth-Sci. Rev. *204*, 103171. https://doi.org/10.1016/j.earscirev.2020.103171.

Brigode, P., Vigoureux, S., Delestre, O., Nicolle, P., Payrastre, O., Dreyfus, R., Nomis, S., Salvan, L., 2021. Inondations sur la Côte d'Azur: Bilan hydro-météorologique des épisodes de 2015 et 2019. LHB *107* (1), 1–14. https://doi.org/10.1080/27678490.2021.1976600.

Caillaud, C., Somot, S., Alias, A., Bernard-Bouissières, I., Fumière, Q., Laurantin, O., Seity, Y., Ducrocq, V., 2021. Modelling Mediterranean heavy precipitation events at climate scale: An object-oriented evaluation of the CNRM-AROME convection-permitting regional climate model. Clim. Dyn. *56* (5), 1717–1752. https://doi.org/10.1007/s00382-020-05558-y.

Caillaud, C., Somot, S., Douville, H., Alias, A., Bastin, S., Brienen, Demory, Dobler, Feldmann, Frisius, Goergen, Kendon, Keuler, Lenderink, Mercogliano, Pichelli, Soares, Tolle, & de Vries. (2023). Mediterranean Heavy Precipitation Events in a warmer climate: Robust versus uncertain changes with a large convection-permitting model ensemble. ⟨https://scholar.google.com/citations?view_op=view_citation&hl=fr&user=wG2YZ9EAAAAJ&sortby=pubdate&citation_for_view=wG2YZ9EAAAAJ:sxPTjD2EoucC⟩.

Ceresetti, D. (2011). *Space-time structure of heavy rainfall events*: *Application to the Cévennes-Vivarais region.* Université Joseph-Fourier - Grenoble I.

Ceresetti, D., Ursu, E., Carreau, J., Anquetin, S., Creutin, J.D., Gardes, L., Girard, S., Molinié, G., 2012. Evaluation of classical spatial-analysis schemes of extreme rainfall. Nat. Hazards Earth Syst. Sci. *12* (11), 3229–3240. https://doi.org/10.5194/nhess-12-3229-2012.

Chmiel, M., Godano, M., Piantini, M., Brigode, P., Gimbert, F., Bakker, M., Courboulex, F., Ampuero, J.-P., Rivet, D., Sladen, A., Ambrois, D., Chapuis, M., 2022. Brief communication: Seismological analysis of flood dynamics and hydrologically triggered earthquake swarms associated with Storm Alex. Nat. Hazards Earth Syst. Sci. *22* (5), 1541–1558. https://doi.org/10.5194/nhess-22-1541-2022.

Chochon, R., Martin, N., Lebourg, T., & Vidal, M. (2021). Analysis of extreme precipitation during the mediterranean event associated with the Alex storm in the Alpes-Maritimes : Atmospheric mechanisms and resulting rainfall. 17.

Delrieu, G., Nicol, J., Yates, E., Kirstetter, P.-E., Creutin, J.-D., Anquetin, S., Obled, C., Saulnier, G.-M., Ducrocq, V., Gaume, E., Payrastre, O., Andrieu, H., Ayral, P.-A., Bouvier, C., Neppel, L., Livet, M., Lang, M., du-Châtelet, J.P., Walpersdorf, A., Wobrock, W., 2005. The catastrophic flash-flood event of 8–9 september 2002 in the gard region, France: a first case study for the Cévennes–Vivarais Mediterranean hydrometeorological observatory. J. Hydrometeorol. *6* (1), 34–52. https://doi.org/10.1175/JHM-400.1.

Drobinski, P., Ducrocq, V., Arbogast, P., Basdevant, C., Bastin, S., Beguery, L., Belamari, S., Béranger, K., Bock, O., Bouin, M.-N., Boudevillain, B., Bousquet, O., Bouvier, C., Braud, I., Calvet, J.-C., Champollion, C., Chanzy, A., Claude, M., Cocquerez, P., Vandervaere, J.-P., 2013. HyMeX, le cycle de l'eau méditerranéen à la loupe. La MétéOrol. *80*, 23–36. https://doi.org/10.4267/2042/48792.

Ducrocq, V., Braud, I., Davolio, S., Ferretti, R., Flamant, C., Jansa, A., Kalthoff, N., Richard, E., Taupier-Letage, I., Ayral, P.-A., Belamari, S., Berne, A., Borga, M., Boudevillain, B., Bock, O., Boichard, J.-L., Bouin, M.-N., Bousquet, O., Bouvier, C., Tamayo, J., 2014. HyMeX-SOP1: the field campaign dedicated to heavy precipitation and flash flooding in the northwestern Mediterranean. Bull. Am. Meteorol. Soc. *95* (7), 1083–1100. https://doi.org/10.1175/BAMS-D-12-00244.1.

Dufeu, E., Mougin, F., Foray, A., Baillon, M., Lamblin, R., Hebrard, F., Chaleon, C., Romon, S., Cobos, L., Gouin, P., Audouy, J.-N., Martin, R., Poligot-Pitsch, S., 2022. Finalisation de l'opération HYDRO 3 de modernisation du système d'information national des données hydrométriques. LHB *108* (1), 2099317. https://doi.org/10.1080/27678490.2022.2099317.

EEA. (2016). European digital elevation model (EU-DEM) [Jeu de données]. ⟨https://sdi.eea.europa.eu/catalogue/srv/api/records/d08852bc-7b5f-4835-a776-08362e2fbf4b⟩.

Emmanuel, I., Andrieu, H., Leblois, E., Janey, N., Payrastre, O., 2015. Influence of rainfall spatial variability on rainfall–runoff modelling: benefit of a simulation approach? J. Hydrol. *531*, 337–348. https://doi.org/10.1016/j.jhydrol.2015.04.058.

Ficchì, A., Perrin, C., Andréassian, V., 2016. Impact of temporal resolution of inputs on hydrological model performance: an analysis based on 2400 flood events. J. Hydrol. *538*, 454–470. https://doi.org/10.1016/j.jhydrol.2016.04.016.

Garambois, P.A., Larnier, K., Roux, H., Labat, D., Dartus, D., 2014. Analysis of flash flood-triggering rainfall for a process-oriented hydrological model. Atmos. Res. *137*, 14–24. https://doi.org/10.1016/j.atmosres.2013.09.016.

Gaume, E., Borga, M., Llassat, M.C., Maouche, S., Lang, M., Diakakis, M., 2016. Mediterranean extreme floods and flash floods. The Mediterranean Region under Climate Change. A Scientific Update, 133-144..

Gilabert, J., Llasat, M.C., 2018. Circulation weather types associated with extreme flood events in Northwestern Mediterranean. Int. J. Climatol. *38* (4), 1864–1876. https://doi.org/10.1002/joc.5301.

IGEDD. (2023). Retour d'expérience des intempéries des 2 et 3 octobre 2020 dans les Alpes-Maritimes—Enseignements de la crise et propositions pour une reconstruction résiliente. ⟨https://www.igedd.developpement-durable.gouv.fr/retour-d-experience-des-intemperies-des-2-et-3-a3155.html⟩.

Lengfeld, K., Walawender, E., Winterrath, T., Becker, A., 2021. CatRaRE: A Catalogue of radar-based heavy rainfall events in Germany derived from 20 years of data. Meteorol. Z. 469–487. https://doi.org/10.1127/metz/2021/1088.

Llasat, M.C., Llasat-Botija, M., Prat, M.A., Porcú, F., Price, C., Mugnai, A., Lagouvardos, K., Kotroni, V., Katsanos, D., Michaelides, S., Yair, Y., Savvidou, K., Nicolaides, K., 2010. High-impact floods and flash floods in Mediterranean countries: the FLASH preliminary database. Adv. Geosci. *23*, 47–55. https://doi.org/10.5194/adgeo-23-47-2010.

Mélèse, V., Blanchet, J., Molinié, G., 2018. Uncertainty estimation of intensity–duration–frequency relationships: a regional analysis. J. Hydrol. *558*, 579–591. https://doi.org/10.1016/j.jhydrol.2017.07.054.

Molinié, G., Ceresetti, D., Anquetin, S., Creutin, J.D., Boudevillain, B., 2012. Rainfall regime of a mountainous Mediterranean region: statistical analysis at short time steps. J. Appl. Meteorol. Climatol. *51* (3), 429–448. https://doi.org/10.1175/2011JAMC2691.1.

Nuissier, O., Joly, B., Joly, A., Ducrocq, V., Arbogast, P., 2011. A statistical downscaling to identify the large-scale circulation patterns associated with heavy precipitation events over southern France. Q. J. R. Meteorol. Soc. *137* (660), 1812–1827. https://doi.org/10.1002/qj.866.

Payrastre, O., Nicolle, P., Bonnifait, L., Brigode, P., Astagneau, P., Baise, A., Belleville, A., Bouamara, N., Bourgin, F., Breil, P., Brunet, P., Cerbelaud, A., Courapied, F., Devreux, L., Dreyfus, R., Gaume, E., Nomis, S., Poggio, J., Pons, F., Sevrez, D., 2022. The 2 October 2020 Alex storm in south-eastern France: a contribution of the scientific community to the flood peak discharges estimation. LHB *0* (0), 2082891. https://doi.org/10.1080/27678490.2022.2082891.

Qiu, J., Zhao, W., Brocca, L., Tarolli, P., 2023. Storm Daniel revealed the fragility of the Mediterranean region. Innov. Geosci. *1* (3). https://doi.org/10.59717/j.xinngeo.2023.100036 (100036-2).

Ribes, A., Thao, S., Vautard, R., Dubuisson, B., Somot, S., Colin, J., Planton, S., Soubeyroux, J.-M., 2019. Observed increase in extreme daily rainfall in the French Mediterranean. Clim. Dyn. *52* (1), 1095–1114. https://doi.org/10.1007/s00382-018-4179-2.

Ricard, D., Ducrocq, V., Auger, L., 2012. A climatology of the mesoscale environment associated with heavily precipitating events over a northwestern Mediterranean Area. J. Appl. Meteorol. Climatol. *51*, 468–488. https://doi.org/10.1175/JAMC-D-11-017.1.

Rysman, J.-F., Lemaître, Y., Moreau, E., 2016. Spatial and temporal variability of rainfall in the Alps–Mediterranean Euroregion. J. Appl. Meteorol. Climatol. *55* (3), 655–671. https://doi.org/10.1175/JAMC-D-15-0095.1.

Saint-Martin, C., Javelle, P., Vinet, F., 2018. DamaGIS: a multisource geodatabase for collection of flood-related damage data. Earth Syst. Sci. Data *10* (2), 1019–1029. https://doi.org/10.5194/essd-10-1019-2018.

Tabary, P., Dupuy, P., L'Henaff, G., Gueguen, C., Moulin, L., Laurantin, O., & Merlier, C. (2012). A 10-year (1997–2006) reanalysis of quantitative precipitation estimation over France: methodology and first results. International « Wheater Radar and Hydrology », Exeter,IAHS.

Tarboton, D.G. (1989). The analysis of river basins and channel networks using digital terrain data [Thesis, Massachusetts Institute of Technology]. ⟨https://dspace.mit.edu/handle/1721.1/39956⟩.

Tramblay, Y., Somot, S., 2018. Future evolution of extreme precipitation in the Mediterranean. Clim. Change *151* (2), 289–302. https://doi.org/10.1007/s10584-018-2300-5.

Vinet, F., Lumbroso, D., Defossez, S., Boissier, L., 2012. A comparative analysis of the loss of life during two recent floods in France: the sea surge caused by the storm Xynthia and the flash flood in Var. Nat. Hazards *61* (3), 1179–1201. https://doi.org/10.1007/s11069-011-9975-5.